POLITECNICO DI TORINO

Corso di Laurea Magistrale in Ingegneria Energetica e Nucleare

Progettazione e gestione di impianti energetici

1859

Master thesis

Analysis of transfer learning frameworks for thermal dynamics prediction to support the predictive management in buildings

Supervisor:

Prof. Alfonso Capozzoli

Cosupervisor:

Dott. Giuseppe Pinto

Dott. Marco Piscitelli

Candidate:

Riccardo Messina

Academic year 2021/2022

Acknowledgement

To my family,

a special thanks for all sacrifices made to get me here

and the support given to achieve this long desired goal.

Abstract

The huge amount of energy consumption causes serious environmental consequences such as climate change and air pollution, among others, all of which have a significant and negative impacts for humanity and ecosystem survival. The building sector represents one of the most energy intensive field, requiring further attention in order to reduce its environmental impact. Efficient and sustainable buildings have become critical to preserve the environment and will help to reduce the overall amount of energy exploited in buildings, since building inefficiency is one of the primary contributors to global energy consumption, greenhouse gas emissions and, consequently, to the global warming. Machine Learning techniques (ML) and Deep Neural Networks (DNN) are widely acknowledged as an effective way for achieving desired results in prediction tasks, which represent a viable method to expand the use of advanced control strategies for building energy management. However, one of ML shortcomings is related to the amount and quality of training data that strongly limit the application of data-driven models in building energy systems. Most machine learning extrapolation capabilities are insufficient for these strategies, due to their reliance on a large data set that properly characterize the problem. In this perspective, Transfer Learning (TL) has been identified as a promising technique to scale up machine learning approaches. In particular, transfer learning aims to improve the performance of a target learner exploiting knowledge in related environments. Despite its effectiveness, its application in smart buildings

still need further studies. To overcome these limitations, the thesis proposes a statistical investigation on the application of transfer learning to forecast indoor air temperature evolution in buildings. Such technique may help to broaden the use of data-driven models in advanced control strategies, helping the energy sector decarbonization. The case study is represented by a reference medium size office building. Starting from a database of around 1500 EnergyPlus simulations, comparing a Multilayer Perceptron (MLP) and a Long-Short Term Memory (LSTM) neural networks, the last one has been used to predict 1 hour ahead indoor temperature with a granularity of 10 minutes. The analysis helped to quantify the influences of specific features on transfer learning and machine learning performance. In particular, the thesis analyzed both the influence of building specific features such as construction materials, orientation, weather, climate and occupancy as well as data availability and technique on transfer learning performance. Lastly, the resulting outputs have been deeply analyzed to rank the most important features and guidelines on data availability requirements.

Contents

List of Figures

List of Tables

Chapter 1

Introduction

1.1 Building sector energy consumption

Energy sector is the core of contemporary economies and it is essential for society growth and prosperity. Simultaneously, this sector, which is still mainly dominated by the use of fossil fuels in energy production, transformation and usage, accounts for two-thirds of global emissions. CO2 emissions account for roughly 90% of worldwide greenhouse gases (GHG) ones [9], due to the exploitation of fossil fuels like natural gas, oil and coal, as shown in figure1.1:
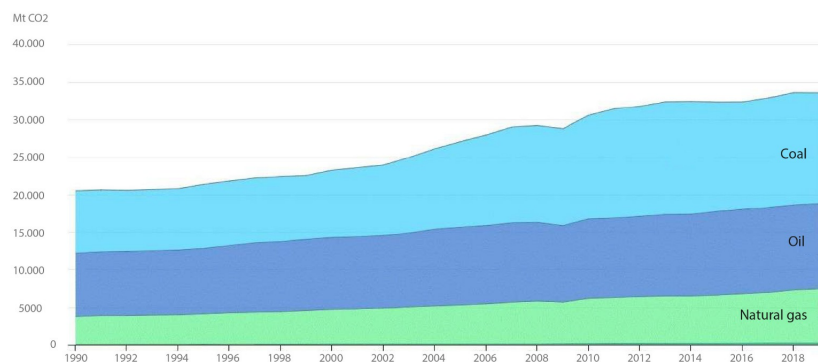
Fig. 1.1: CO2 emission by energy source [1]

.

Emissions coming from the combustion of these sources are the main cause of global warming, that is become one of the principal issue which all word nations are facing in all levels of their infrastructures, industries and economy. The close link between energy usage and climate change has become widely acknowledged. The *Intergovernmental Panel of Climate Change* [10] defined the global warming as the increase of air and sea surface temperatures over the globe. From 2000's building energy demand has grown five times faster than advances in the carbon intensity of power generation [9], and it has significantly increased over the past decades because of an increasing number of households, floor area and the consequently growth of the demand for equipment like air conditioners; Electricity has the potential to become the energy source that people rely on for all of their daily requirements: mobility, cooking, lighting, heating and cooling. Thus, combined with renewable power generation, electrification plays a key part in the energy transition scenario, and electricity reliability and affordability is going to becoming more important regarding people's lives and well-being.[11]. Electricity's contribution to the final energy will rise to almost 35% by 2050, higher respect current 20%. Buildings have contributed significantly to world energy consumption and greenhouse gas emission [12] and it is one of the most energy intensive sector, as shown in figure 1.2. For this reason energy efficient and sustainable buildings have become imperative towards saving the environment. The *Special Report of Global Waring of* $1.5°C$ [10] highlighted the importance of reaching net-zero CO2 emissions avoiding the worst impact of global climate change. 44 countries and the EU have pledged achieving the net-zero emissions target: in total they account for around 70% of global CO2 emissions and Gross Domestic Products (GDP). The *Net Zero By 2050* [2] states that the global electricity demand will increase even more between 2020 and 2050, despite strong growth in renewable energy plants. Thanks to the improving of energy
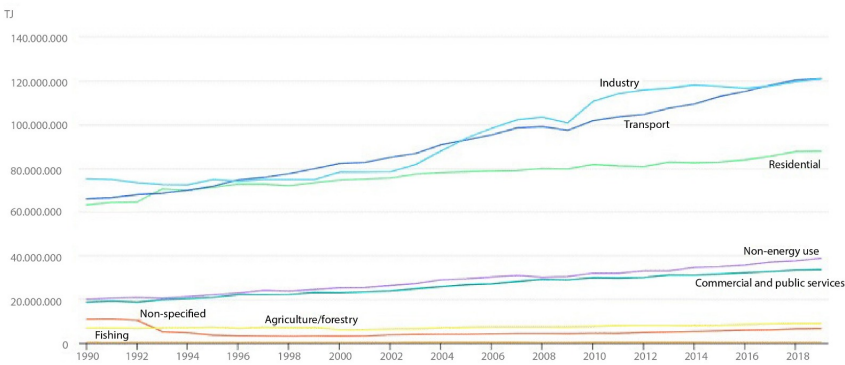
Fig. 1.2: CO2 emission by sector[1].

efficiency, the adoption of renewable energy technologies and the shift to low-carbon electricity, the carbon intensity of the power sector has decreased by more than 90%, while the carbon intensity of end-use sectors has decreased by 65%, and by 2050, energy-related emissions will have dropped by 75%. The predicted consumption by sector is shown in figure 1.3.
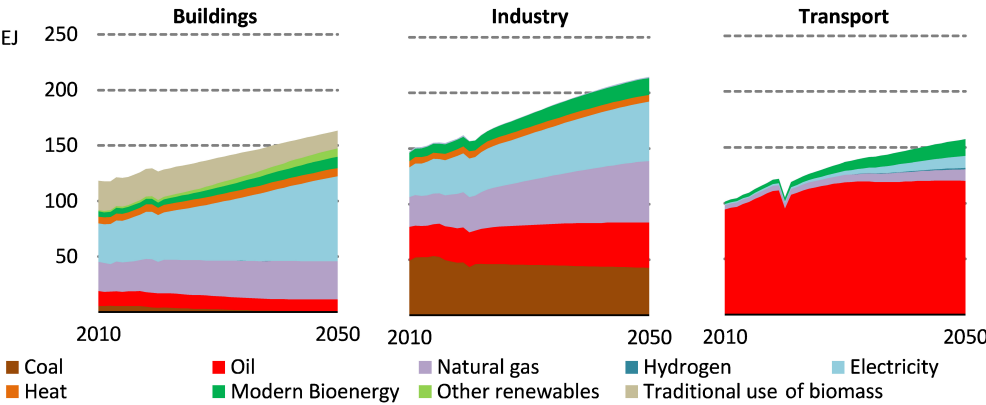
Fig. 1.3: Electricity consumption by sector and source [2].

1.2   Flexibility of buildings energy control systems and smart grid

The decarbonization process faced by the modern society, requires many actions including the introduction of renewable energy systems (RESs) and the management of the energy demand and generation. However, the energy management problem is often complicated by the dependency with weater conditions, user needs, building characteristics and grid constraints, that require advanced control strategy in order to fully exploit the benefits associated to an optimal management. A cost-effective solution, the key to facilitate secure energy control operations and the inclusion of RESs is the *Energy Flexibility*[13]. In energy engineering the term flexibility is described as "the ability to cost effectively balance electricity supply and demand continually maintaining acceptable service quality to connected loads and grid requirements at the same time" [14]. The introduction of a wide amount of renewables in the energy system hard tests the controllability and stability of the grid due to the stochastic nature of production side, which stresses the need for flexibility at demand side. These requirements can be solved thanks to the *Smart grid* concept. A smart grid is defined as an upgradable low voltage electricity distribution network enabled for intelligent control and multidirectional communication between sources, loads and components allowing a cooperative and cheap energy utilization. The smart grid is a connection able to active loads and generators toward a demand side management program, sensors, meters and intelligent coordination systems [14]. The National Institute of Standard Technologies (NIST) define his conceptual grid model as shown in figure 1.4:
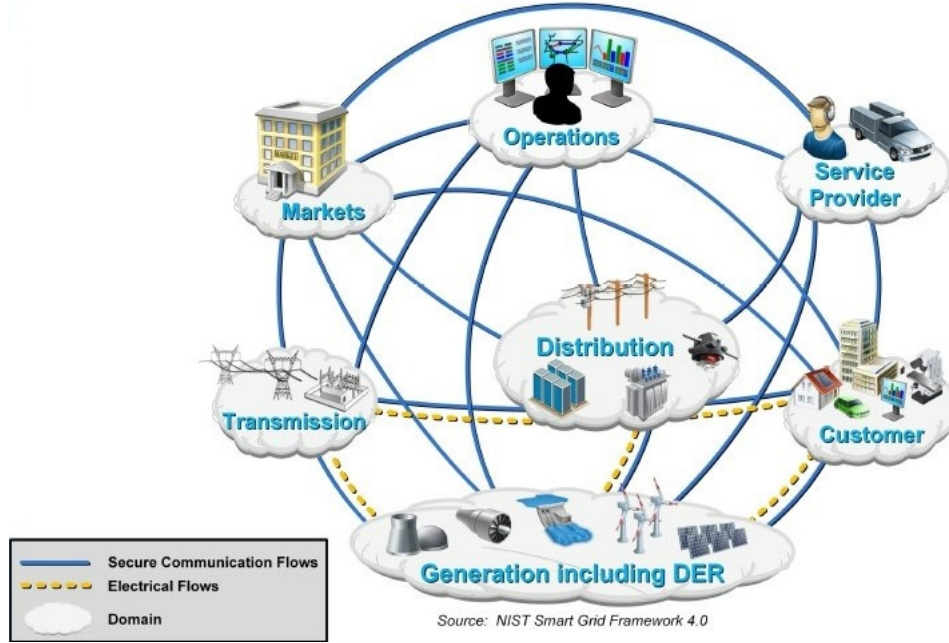
Fig. 1.4: Smart grid NIST conceptual model [3].

Demand-side flexibility management (DSFM) has been proposed and implemented as an effective and sustainable measure to facilitate the penetration of RESs in smart grids. Today's buildings not only consume energy but also produce energy, becoming from energy consumers to energy prosumers and, in the last case, demand-side flexible resources consist of flexible loads, demand-side generations and flexible storage. Building energy flexibility could be achieved by splitting energy demand and energy delivery toward storage that allows to shift energy use from period of high electricity price to period of low electricity price. As mentioned in the NIST [3], these strategies can be implemented thanks to the important concept of *Interoperability* of control systems intended as information exchange between each system devices. Tens of billions of dollars are spent annually on electrical devices and software communications. Beginning with individual sensors and devices found in the home, figure 1.5 shows how the impacts of interoperability can change with the interaction scale.
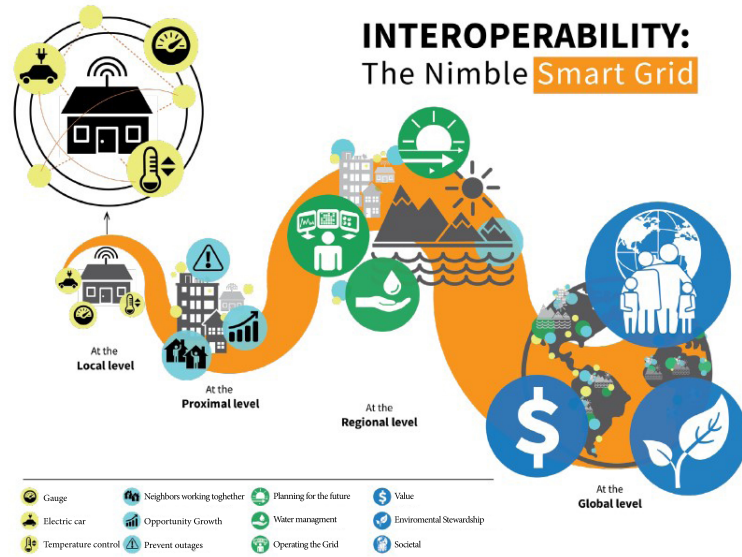
Fig. 1.5: Interoperability across scales [3].

Each level of the diagram represents a new interactions and information exchange. These include:

- **Local**: residential, industrial, and commercial users can benefit from interoperability between individual sensors energy-consuming devices, and system controllers by better monitoring their energy demand (or production) and managing consumption according to their unique needs;

- **Proximal**: customers would be able to communicate with and maybe supply services to their neighbors, aggregators, or distribution utilities if there was interoperability at the community level;

- **Regional**: interoperability at the regional level would increase utilities, system operators, and regulators state awareness, allowing for more efficient operations and better long-term planning. The electrical system's physical interactions with the surrounding environment should also be better handled;

- **Global**: global interoperability will enable wider access to modern energy services, economic development, and environmental preservation on a society scale.

1.3 Control devices

The control of devices need to create these connections is possible through a *Building Energy Management System* (BEMS). BEMSs are computer-based systems that help to manage, regulate, and monitor the building's mechanical and electrical devices such as heating, ventilation, lighting, power systems and, consequently, the energy consumption of the building's equipment [15]. They link the building services plant to a central computer, allowing for management of on/off periods, humidity, and temperatures and so on [16]. The BEMS includes the *Energy Management and Information Systems* (EMIS), which extend and combine the features of a *Building Automation System* (BAS) to analyze and regulate building energy usage and system performance. The EMIS, in turn, contains Energy Information and Fault Detection and Diagnostic (FDD) systems, which are designed to aid decision-making through informative solutions, as well as Automated System Optimization Tools, which modify control settings. Predictive and descriptive modeling are used in Energy Information Systems (EIS) to accomplish tasks such as energy consumption forecasting, anomaly detection, advanced benchmarking, load profiling, and schedule optimization of building energy systems [7]. The Verein Deutscher Ingenieure defines an EMS as "*the proactive, organized and systematic coordination of procurement, conversion, distribution and use of energy to meet the requirements, taking into account environmental and economic objectives*" [4]. The EMS monitors meters, controls building energy consumption and production, while adjusting equipment usage by means of scheduling algorithms. The operation

scheduling problem consists in planning the use of available resources, such as generators and storage, as well as flexible loads, with the aim of minimizing operation costs and/or the environmental impact, while satisfying the energy demand based on systems' inputs such as price. Nowadays, EMS implementation and operations are possible by the growing availability of Internet of Things (IoT) devices and the newest machine learning and deep learning techniques available to deal with huge amounts of data. The EMS has to cooperate with other actors to ensure the correct control of residential devices and consequently the achievement of the aforementioned objectives. Participants of the connection chain are [17]:

a. *energy consumers* that take part in the DR program and they can be either residential, commercial or industrial consumers;

b. a *DR aggregator* that is connected to the customers and executes the DR program;

c. a *Distribution System Operator* (DSO) that controls the distribution grid;

d. an *Independent System Operator* (ISO) or *Regional Transmission Operator* (RTO).

The interconnection between these actors is illustrated in figure 1.6:
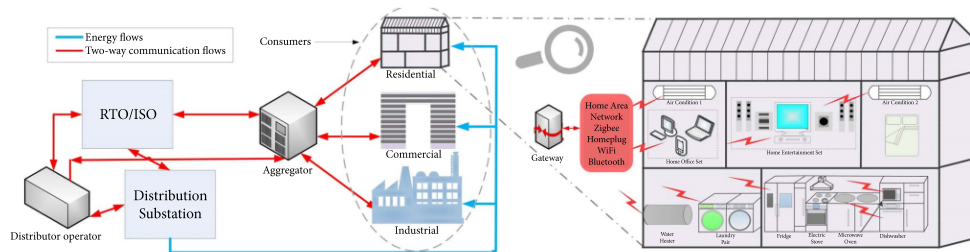
Fig. 1.6: Smart Grid actors [17].

The Demand Response program involves an agreement between utility and consumers. This one can communicate to the utility which are the appliance's loads that it is possible to control, for reaching the targets of program. EMSs, by receiving market and system signals, with a Direct Load Control (DLC), can manage loads such heating, ventilation and air conditioning (HVAC) systems, storage and local generation units, according to user preferences. The main types of EMS control are shown in figure 1.7:
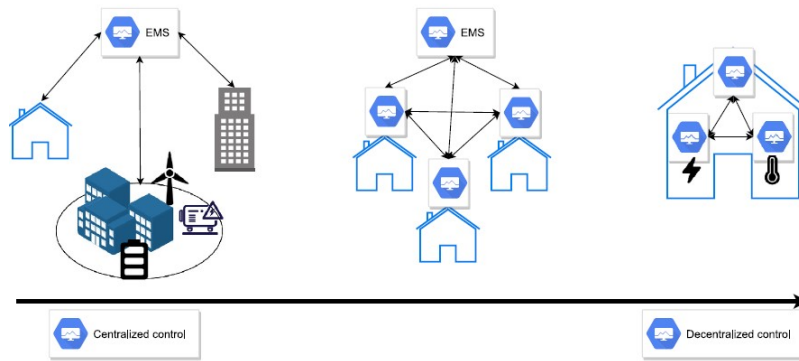
Fig. 1.7: Types of EMS control [4]

Starting form the left of figure 1.7, in a *Centralized Control* the EMS analyzes thermal and electrical loads of a buildings district, without checking every single appliance; in a *Decentralized Control* each dwelling has more owns EMSs, that control their own electric appliances and/or heating system finding the optimal scheduling of all devices and can collaborate between each others and the main grid by exchanging electricity and hot water; in the middle of these two EMS control types, there is another one, according to with each residential unit has its EMS controlling all dwelling loads and can communicate with other EMS's units. The resulting scheduling may be later adjusted by a global controller. The optimization of EMS control can be applied with a Model Predictive Control (MPC). This system is based on the idea of approximating a long-horizon optimal control problem by a short

horizon one. At each time step, the algorithm estimates the future behavior of the system based on current features, and finds an optimal state based on the prediction. Next, new forecasts are available, and the procedure is repeated. In other words, the original optimization problem addresses the forecast uncertainties by sequentially making short-term decision, based on new short-term forecasts [4]. Furthermore, the MPC predicted the behavior of the system under more control strategies and chose to communicate the better one to the consumer's devices. MPC functions are summarized below:

- *Weather predictive/responsive*: the buildings' capacity to predict/respond to external climatic conditions and choose the most appropriate operation profile as a result;

- *User predictive/responsive*: the building's capacity to predict users real-time interactions with the integrated technology, and learning from their behavior.

- *Grid predictive/responsive*: concerns the predictions of building's action/reaction to signals/information from the grid. The goal is maximizing energy/cost efficiency at the district/city scale.

- *Thermal mass predictability/adaptability*: concerns the prediction of building's thermal mass effects based on itself and the building energy loads.

1.4   Machine learning applications in buildings

Buildings dynamics and energy consumption are highly dependent on different building physical, operational, and functional characteristics, as well as meteorological and temporal properties. Building features and energy

performance forecasting helps city and community managers have a better understanding of their future energy needs, and plan to satisfy them more efficiently[5]. Machine learning (ML) has faced an increasing popularity in building energy management due to its capability and flexibility in model development; ML is a set of data-driven techniques able to recognize patterns within input data and predict future variables or perform decision making actions. These techniques have already achieved significant success in many knowledge areas and many articles have been written where features and skills learned from training data could be used to predict future outcomes to improve building performance, occupant comfort and health. In the following figure 1.8, is shown the percentage of papers using building types for Building Energy Performance Forecast (BEPF). Different model

Bldg. Types
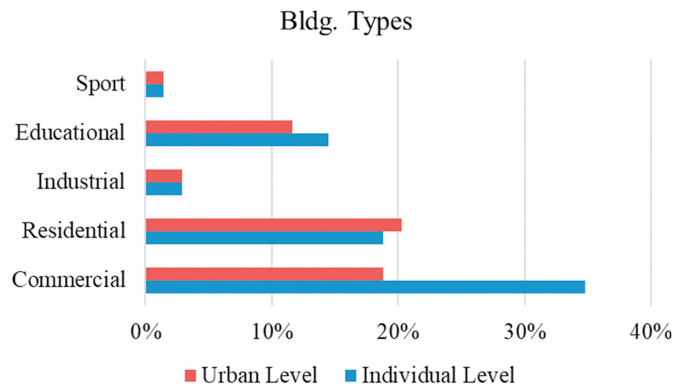
Fig. 1.8: Percentage of papers using various building types for BEPF [5].

types exist, but two categories are predominant. The first one are the *white-box models*, which is detailed physics based methods, regulated by algebraic and differential equations; these models achieve high accuracy, precision and a detailed description of thermal phenomena, but it needs of high computational efforts and it is difficult to calibrate. On the other hand, *black-box models* are data driven methods, that rely on the available historical building data to identify model structure and data relationship. These models are suitable for predicting future behavior under similar set

of conditions. These approaches are able to represent the dynamic of a real system, reducing computational costs while identifying parameters that optimize a given objective function [18], without the need of expert knowledge-based judgment or calibration; but the shortcoming of these models are the absence of physical representation and the misunderstanding user side concern how operate the model. The ideal scenario of machine learning is the availability of a lot of labeled training data and similarity between training and testing features space, because if there are some differences, the prediction could be discounted, but, at the same time, uncertainty is an unavoidable part of model outputs behavior. Another problem that leads to the failure of the predictions is the lack of historical data or the limitation in installing additional meters for monitoring building features. To overcome these limitations, the thesis analyze the applications of *Transfer Learning* in smart buildings, with the aim to represent building thermal dynamics.

1.5 Thesis contributions and structure

The goal of this study is to assess the effectiveness of transfer learning for building thermal dynamics in several deployment conditions. This is done developing a LSTM that has to map and generalize the relationships between all features regarding indoor and outdoor environment, as temperature, occupancy, solar radiation, HVAC ventilation air mass flow rate or efficiency. In this way LSTM can be applied to different environments, despite several indoor and outdoor conditions, as well as the building use and function. Successively, part of a database of around 1500 EnergyPlus simulations was exploited to run machine learning (ML) and transfer learning (TL) simulations. The aim is to create a lot of different environments, based on several occupancy profile, climate file, HVAC system efficiency or zone, useful to test and demonstrate the potential and the effectiveness of TL technique

in the building environment. Results aim to discuss the most influencing factor on the effective deployment of transfer learning, suggesting future guidelines for the application of such technique. The thesis is structured as follow:

- **Chapter 2**: concerns the description of the machine learning techniques exploited in this thesis work; in particular, starting from the explanation of the NN mechanisms as feed forward and recurrent neural network, following with the description of NNs used and the transfer learning concept;

- **Chapter 3**: describes the case study and the creation process of the data set used, the different occupancy, MELs lighting profiles related each others, the climate file and the HVAC efficiency levels. Next will be shown the variables outcome from the simulations and the relationship between some of these and the building energy consumption;

- **Chapter 4**: deals with the selection of features used to train the models, following with the description of exploited NNs structures, the tuning and optimization of them hyperparameters. Next deployed cases are shown and metrics useful to evaluate the goodness of results are described;

- **Chapter 5**: concerns the evaluation of the produced outcomes and metrics cited previously with the discussion of the obtained results;

- **Chapter 6**: deals with conclusive observation and prospective future projects.

Chapter 2

Neural networks and Transfer Learning concept

Artificial neural networks (ANNs) are machine learning techniques exploited for learning, optimizing and generalizing the relationship between linear and non-linear data. Their concept exist just from some decades, but to manage them, more computational power and resources need, that are available and accessible nowadays, so it is possible to apply them to a huge amount of data and several types of applications. ANNs structure is designed to replicates how biological organisms learn. Neurons are cells that make up the human nervous system, by means axons and dendrites, that link neurons with connections called synapses, whose response changes based on external stimuli. Each neuron elaborate inputs by means an activation function, scaling them by a weight, which connected each neuron to the next one.

2.1 Neural network mechanisms

2.1.1 Feed Forward neural networks

The *Perceptron* is the simplest type of neural network. As shown in figure 2.1, it is composed by a single input layer, from which the information is send to the output node, as shown in figure 2.1. This one applies a linear
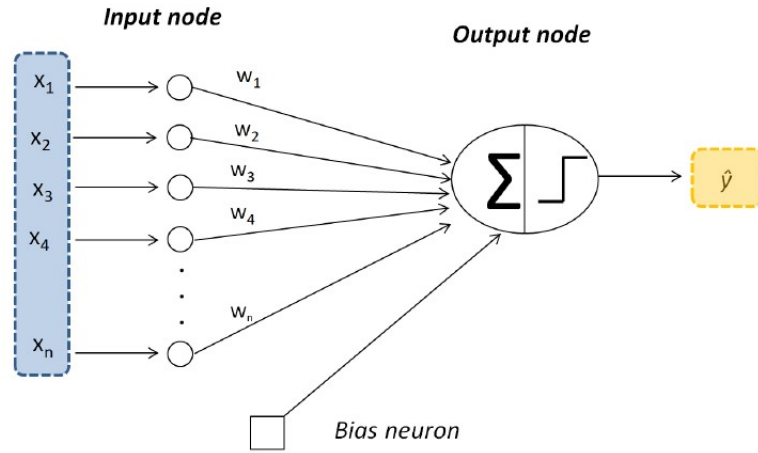
Fig. 2.1: Perceptron architecture [6].

activation function and add a bias b and a weight w to each neuron input; b and w are related by the function 2.1.

$$y = \sum_{t=0}^{n} w_i xi + b \qquad (2.1)$$

Several activation functions can be applied inside a net, based on the model type to simulate. Deep Neural Networks are usually exploited; they are composed by multiple layers, more than simple perceptron net. More specifically, in this project a MLP (Multilayer Perceptron) and a LSTM (Long-Short Term Memory) are compared, being respectively artificial feedforward and recurrent neural networks (ANN and RNN). Layers between input and output ones are known as *hidden layers*, since the calculations conducted are not apparent to the user. *Feedforward* Networks are called that because of their design within successive layers feed into one another in

the forward direction, from the first (input) to the last layer (output), from the left to the right side [6]. An example of more complex neural network structure (respect to the perceptron one) is shown in figure 2.2:
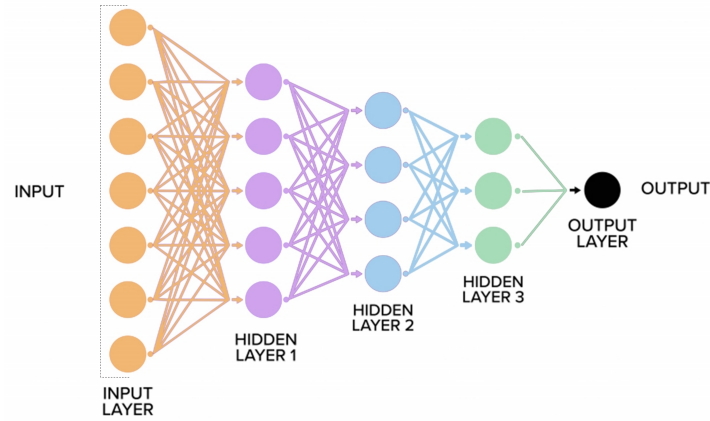
Fig. 2.2: Deep neural Network structure example.

To reach high prediction accuracy, the model needs of a training phase, during which, by a supervised learning approach (schematically illustrated in figure 2.3), the net learn the relationship between input features and true outcomes, minimizing the prediction error, also known as *Loss function*.
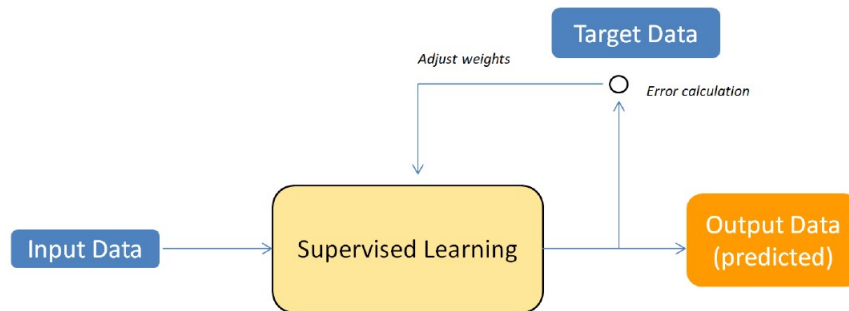
Fig. 2.3: Supervised learning schema [6].

Thus, training concerns the update of weights and biases given to the features in order to produce output values reaching high prediction performance. This is an iterative mechanism known as *Forward Propagation*, concerning error computation, and *Backpropagation*, concerning biases and weights

adjustment. All that allow to fit network hyperparameters; these ones are variables like the learning rate, the number of epochs, the number of hidden layers and neurons within each of these and the activation function, which affect weights and bias.

2.1.2 Recurrent neural networks

Recurrent neural networks (RNNs) are highly exploited for sequential data processing, as the case of time series forecasting issue. These NN types differentiate respect the simple feed forward networks, principally because layers not work independently, but there is an exchange of information across them. This is possible thanks to *Backpropagation through time*, more complex respect to the standard backpropagation, because at each time step the loss function (between predicted and real values) and the gradients of total loss with respect to network's parameters are computed. This process goes in the opposite way respect the feed forward direction, so from the right to the left. This parameter sharing is suitable because allows the user to generalize the network and apply it to cases of different fields. This mechanism is shown below, in figure 2.4:
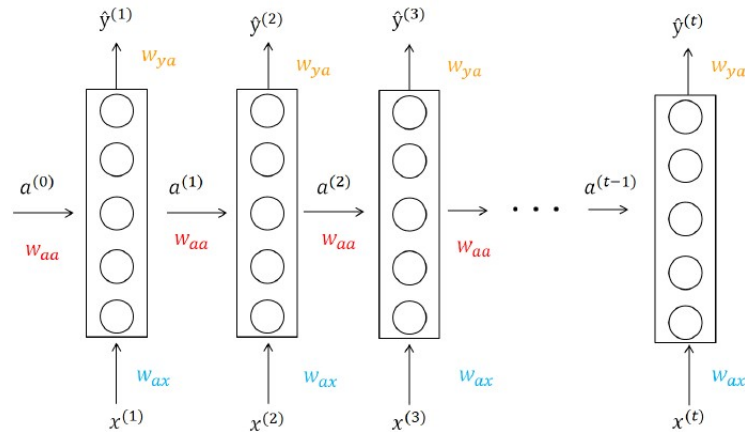
Fig. 2.4: RNNs structure [6].

RNN transfers an activation function to the next layer at each time step; the first activation is usually set to zero or randomly. Information is exchanged through activation, RNN scans the data from left to right, and its predictions are based not just on current input but also on previous ones. This process can be mathematically explained as follow:

$$a^{(1)} = g_1(w_{aa}a^{(0)} + w_{ax}x^{(1)} + b_a) \tag{2.2}$$

$$\hat{y}^{(1)} = g_2(w_{aa}a^{(0)} + w_{ax}x^{(1)} + b_a) \tag{2.3}$$

2.2   Multilayer perceptron

Multi-layer Perceptron (MLP) is a supervised learning algorithm. As shown in figure 2.5, MLP is composed by an input and an output layer with one or more hidden layers between them.
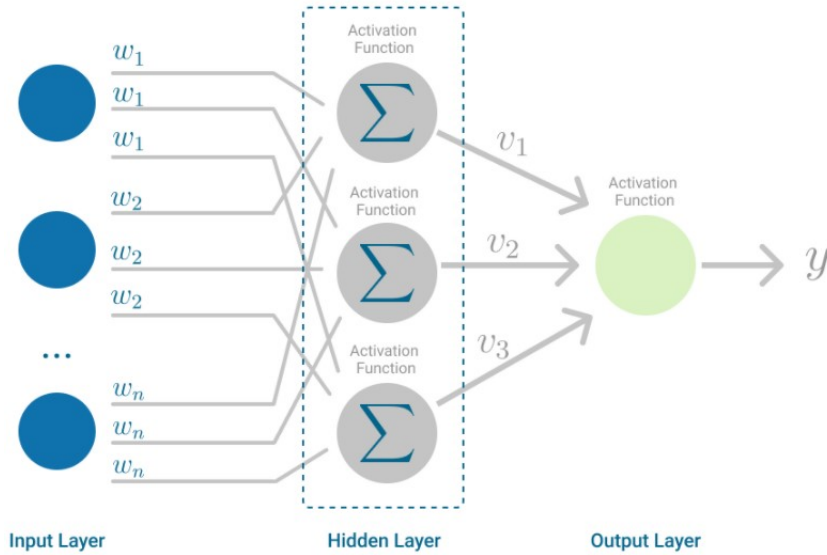
Fig. 2.5: MLP structure.

MLP is a neural network where the mapping between inputs and outputs is non-linear. Multilayer Perceptron can use any activation function like ReLU or sigmoid. It falls under the category of feedforward algorithms,

because inputs are combined with the initial weights in a weighted sum and subjected to the activation function, just like in the Perceptron; but the difference is that each linear combination is propagated to the next layer, so the information move in only one direction. Backpropagation is the learning mechanism that allows the Multilayer Perceptron to iteratively adjust the weights in the network, with the goal of minimizing a certain cost function. Backpropagation needs a requirement to work properly: the function that combines inputs and weights in a neuron, for instance the weighted sum, and the threshold function, for instance ReLU, must be differentiable.

2.3 Long Short Term Memory

Long Short-Term Memory (LSTM) is an artificial *Recurrent Neural Network* (RNN) architecture used in deep learning field. LSTM has feedback connections and it is able to process entire sequences of data, learning long-term dependencies. For example, LSTM is applicable to tasks such as unsegmented, connected handwriting recognition, speech recognition and anomaly detection in network traffic or intrusion detection systems (IDSs). LSTM networks are well-suited to classifying, processing and making predictions based on time series data. An RNN using LSTM units can be trained with a supervised model, on a set of training sequences, using an optimization algorithm, like gradient descent, combined with backpropagation through time to compute the gradients needed during the optimization process; in this way, each weight of the LSTM network changes in proportion to the error derivative (at the output layer of the LSTM network) with respect to corresponding weight. The principal property of a LSTM is to remember useful information and forget irrelevant ones. This is allowed thanks to a specific gating mechanism and a structure composed by:

- *Hidden state*, managing the short term memory;

- *Cell state*, managing the long term memory and dependencies.

LSTM scheme is shown in figure 2.6:
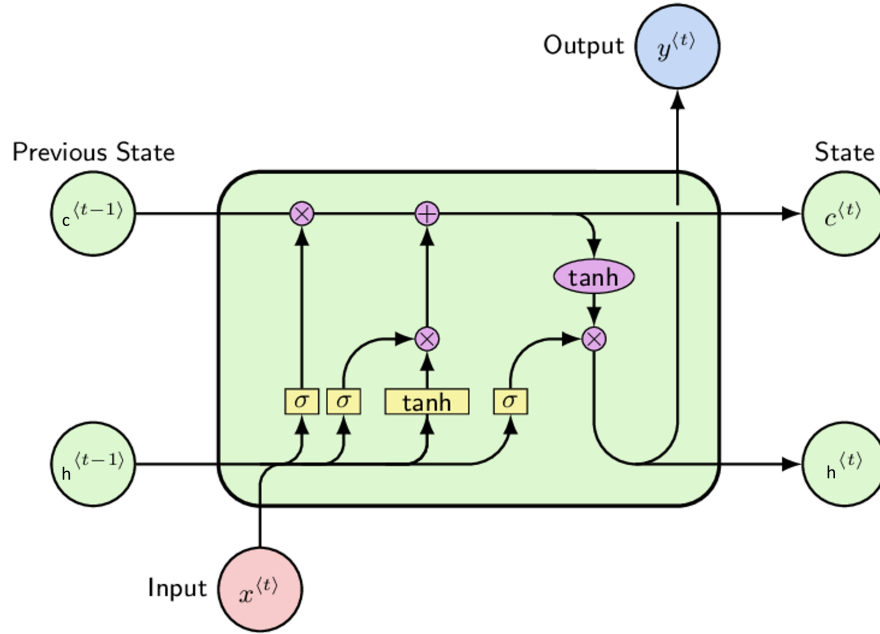
Fig. 2.6: LSTM scheme.

Memory cells, in particular, employ gates to govern the information to be preserved or discorded at each time step before carrying on the long and short term information to the next cell gates; this system filters out unnecessary data. Cell state proceeds in a straight line throughout the series, with very slightlinear interactions. The LSTM may delete or add information to the cell state, which is carefully controlled by structures called gates; these ones are a mechanism to selectively allow information to carry on across the LSTM layer. A sigmoid neural net layer plus a pointwise multiplication operation make them up. The sigmoid layer produces integers from zero to one, indicating how much of each component should be allowed to pass. A value of zero indicates that the component is irrelevant and may be eliminated, whereas a value of 1 indicates that the component is critical and must be preserved. Proceeding in steps, the LSTM data

process develops in three phases as soon as the number of gates. The first step concerns what information will be removed from the cell state, which regulate the information flow into and out of the cell. The "*forget gate*", a sigmoid layer, makes this judgment. Next, another sigmoid layer, the *input gate*, determines what new data will be updated in the cell state; at the same time a *tanh* layer creates a vector of new candidate values, which are elementwise multiplicated with values previously selected by the input gate, generating a new vector with the goal of update the cell state. The last step is divided into two strides: first of all another sigmoid layer, the *output gate* determines which aspect of the cell state will be output, and then the cell state passes through a *tanh* and multiplied by the outcoming from the sigmoid layer.

2.4 Sequence to sequence RNN types

According to the problem to be addressed, different types of RNNs architecture can be implemented. Their are defined as *Sequence to Sequence* RNNs because of the shape of input and output variables, that are series of one or more values. It is possible to distinguish five different structures, as shown in figure 2.7:
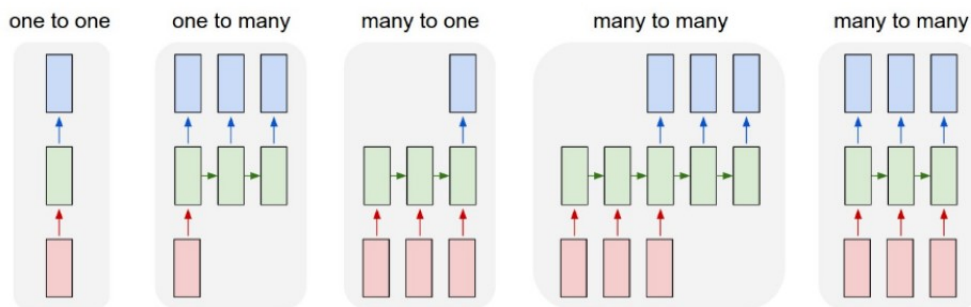
Fig. 2.7: Types sequence to sequence RNN configurations.

In this study a Many to Many configuration is exploited, which gives in

output a sequence of predicted values for each input features sequence. About input and output variables, chapters 3 and 4 will deal with better.

2.5   Literature review on ML techniques for building dynamics

In the recent decade, ML techniques for building dynamic modeling has gotten more attention by means the increasing computational power, use of sensors and meters. Thus, nowadays is possible to exploit data collected trough efficient artificial neural network models. Moreover, these ones are useful for their ability to deal with non-linear, multi-variable data set, despite these can rapidly lose accuracy when data have a variable distribution over time. Machine learning applications have seen multiple applications in predicting the internal temperature of buildings. One of these is the work performed by Xu et al. [19], who applied a DL method to predict indoor air temperature one step ahead and multi-time step ahead to test and compare performance between two LSTM models, one of which is modified by an error correction. Results demonstrate that novel LSTM model overcomes the standard one, improving predicted data precision. Another interesting study is published by Shi et al. [20] in a tobacco manufacturing warehouse in Chongqing. This study provides a model based on BP neural networks applied on a cloud database to forecast indoor relative humidity and air temperature concurrently every 10 minutes, 6 hours, 24 hours, and 72 hours in advance. The advantage of the online database is avoid the exploitation of some features like solar radiation, thermodynamic properties of building materials, or wind speed, allowing a less complex model with good performances for each forecast horizon. In 2021, Sun et al. [21] proposed a multiple linear regression model to predict the supply temperature, adjusting it according to the feedback of the consumers' set

point and actual indoor temperature deviation. These data were sharing by wireless collection devices installed in the building served by a CHP units and peak shaving boilers. The results showed an heat consumption saving of 6% in the heating stations and that control period changes based on thermal heating method and building thermal characteristics. Ellis et al. [22] used an Encoder-Decoder LSTM to simulate an air handling unit-variable air volume (AHUVAV) HVAC system. Forecasts were employed by an MPC to optimize energy costs, exploring its performance through E+ software. Another interesting work was performed by Mtibaa et al. [23] that applied a multi-step ahead IAT prediction in a multi-zone building comparing a Multilayer Perceptron (MLP), a Non-linear Autoregressive model with exogenous inputs (NNARX) and two sequence-to-sequence LSTM models: a LSTM-MISO (Multi-Input Single-Output) and a LSTM-MIMO (Multi-Input Multi-Output), both applied on real smart buildings, one using a Variable Air Volume (VAV) and the other one a Constant Air Volume (CAV) HVAC system. Results proved that LSTM-MIMO is the best method for modeling IAT for both VAV and CAV buildings. Fang et al. [24] proposed three LSTM-based sequence to sequence model architectures to make a multi-step ahead IAT forecasting: a LSTM-Dense model, a LSTM-LSTM model and a LSTM-dense-LSTM model, evaluating the performance under different forecast horizons. In this paper results were compared with two benchmarks: a Naive model and a Prophet model (developed by Facebook [25]). Results analyses showed that the LSTM-dense model performs better for shorter forecast horizons, while the other two architecture models are more suitable for longer forecast horizons, but all of LSTM-based models overcome the two benchmarks. Moreover, a study which concerns something similar to the models pre-processing done in this thesis, was performed by Afroz et al. [26], where, in the context of thermal comfort, this study examines real indoor environmental data to predict IAT in multiple adjacent

zones in a commercial building with the aim of resetting the air temperature set-point without affecting occupant comfort. A NNARX is exploited for single-zone and multi-zone prediction, optimizing the model performance changing more features as network size, optimal input parameters or size of training data. As a result, they obtained better performance, easing the application to real systems, complexity of the model structure, minimum features exploited and energy savings.

2.6   Transfer learning concept

Machine learning techniques are increasingly using for different application of building field such as occupancy detection and activation recognition, building load prediction, energy system control and building dynamics modeling and forecasting, which is the main issue of this project. Traditionally, before applying forecasting, a neural network have to learn knowledge between data; it is made by diving the whole data set in three sub-datasets: training, validation and test data set, going ahead with the respective phases. The training phase is the one during which the net carries out some adjustments to the weights applied to input data, through an activation function and an optimization techniques, comparing the outputs with the real values. Then the validation phase concerns in a small part of data set with which the net is tested and it is possible to understood the forecasting accuracy; if it is not satisfying, the net is trained again. Ones net performance are good, the testing phase is the next one and consists in the real application of forecasting. Until nowadays, building dynamic forecasting is made training the net on data monitoring during the building life. The shortcoming of this method is the need of a certain amount of data to ensure good forecasting performance. So at the beginning of building life it is not possible to apply automated energy savings strategies by forecasting. For this reason, *Trans-*

fer Learning (TL) is the optimal solution. According to TL, when strategies have to be applied to a new building, called *Target Building*, or after an energy requalification, a similar one is identified, called *Source Building*. A "similar" building can have equal climate, energy efficiency, HVAC system or final uses. The advantage of TL is the availability of great amount of source building data, on which the net could be trained to learn knowledge between features; weights of the net are saved and then applied to the target building data. In this way it is possible to achieve building dynamic forecast from the birth of the target building or shortly thereafter. Transfer learning can be classified according to several aspects, but before describing them, let's explain better the definition of *Domain, Task* and *Transfer Learning*:

- A *Domain D* is composed by two components: a feature space χ and a probability distribution $P(X)$, where $X = x_1, ..., x_n \in \chi$;

- A *Task $\mathcal{T}$* is composed by two components: a label space Y and a predictive function $f(\cdot)$, which is learned from the training data, represent by pair x_i, y_i, where $x_i \in \chi$ and $y_i \in Y$. The function $f(\cdot)$ need to approximate the conditional probability $P(y|x)$ and improve the forecasting accuracy.

- *Transfer learning.* Given a source domain D_S and task $\mathcal{T}_s$, a target domain D_T and task $\mathcal{T}_T$, transfer learning helps to improve the learning of the target predictive function in D_T using the knowledge in D_S and $\mathcal{T}_S$, where $D_S \neq D_T$ and $\mathcal{T}_S \neq \mathcal{T}_T$ [7].

Now it is possible to describe how transfer learning can be categorized, based on different characteristics. The first one is based on the similarity between source and target task and domain:

- In the *Inductive Transfer Learning* the source task and the target task are different ($\mathcal{T}_S \neq \mathcal{T}_T$), while source and target domain can be equal

or different. The goal of this case is helping the learning of the target predictive function $f(\cdot)$ in D_T exploiting data in D_S, ($\mathcal{T}_S$ and part of labeled data in D_T).

- In the *Transductive Transfer Learning* source task is equal to target task ($\mathcal{T}_S = \mathcal{T}_T$) and source and target domain are different ($D_S \neq D_T$).

- In the *Unsupervised Transfer Learning* no labeled data are available in source and target domain and target task is different but related to source task ($\mathcal{T}_S \neq \mathcal{T}_T$).

Another categorization of TL is based on the strategy using to share knowledge. According to it, let's distinguish four approaches:

- According to the *Instance-based TL*, a part of source domain data D_S is used for learning in target domain D_T when historical target task data are available. It is made by reweighting source domain data helping learning in target domain.

- According to the *Feature representation-based TL*, features are exploited to maps instances from source and target domains improving training on target task.

- According to the *Model parameter-based TL*, source and target task share parameters or model hyper-parameters distribution.

- According to the *Relational knowledge-based TL*, relationship among source and target domain data is similar and it is transferred among data.

An illustration of this classification is shown in figure 2.8, referring to the building load prediction:
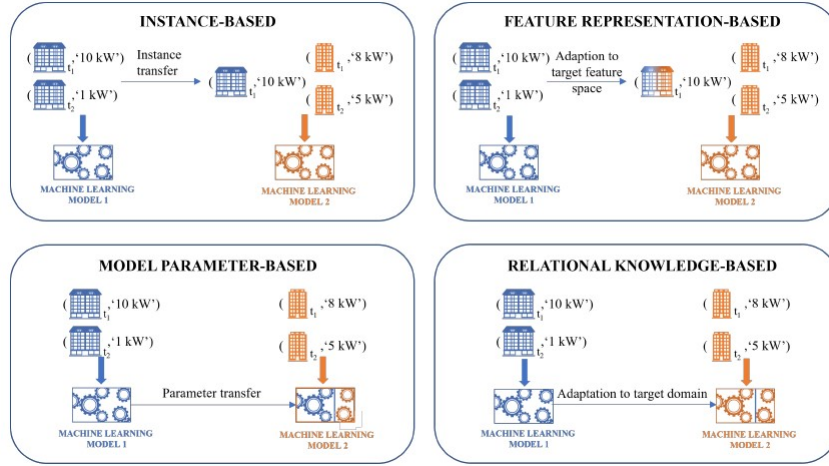
Fig. 2.8: TL classification approaches [7].

In this project, the TL approach adopted is the Model Parameter-based. This one can be applied in two different ways:

1. *Features extraction* concerns the NN training on the source domain data applying then model, with saved weights, directly on the target domain data, fine tune just some layers of the net with the limited amount of target data and freeze the other ones, in such a way to adapt the model to the target building.

2. *Weights initialization* concerns the NN training on the source domain data and subsequently a retrain of the whole network on target domain data. This approach aim to initialize the weights and adapt better the model to the target data.

A representation of these two cases are shown in figure 2.9: The last classification of TL, it is related to the similarity between source and target space; in particular let's distinguish:

- *Heterogeneous TL* if the feature and label spaces are different ($\chi_S \neq \chi_T$ and $Y_S \neq Y_T$);
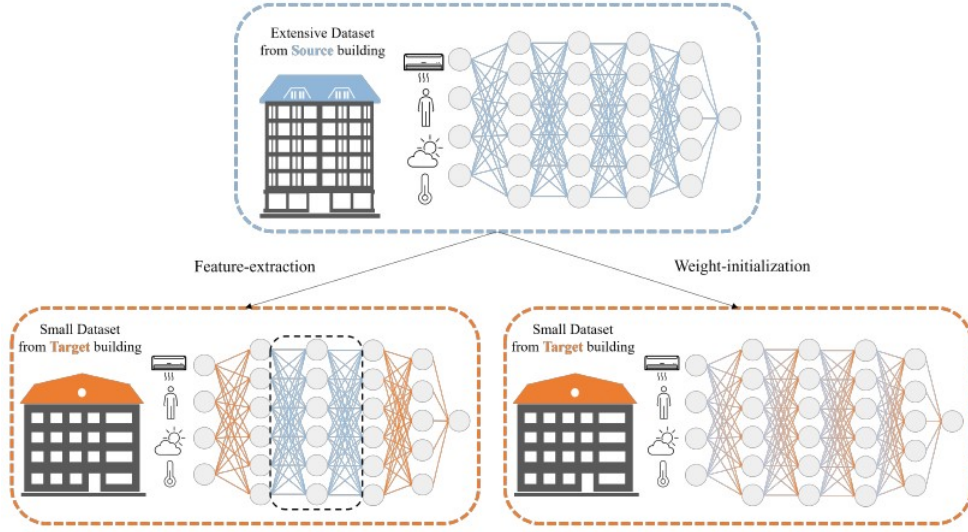
Fig. 2.9: Feature extraction and weight initialization examples [7].

- *Homogeneous TL* if the feature and label spaces are the same ($\chi_S = \chi_T$ and $Y_S = Y_T$).

Understood the amount of aspects characterizing TL typologies, it is interesting notice an overview of TL applications related to the techniques used to execute them. Pinto et al. [7] presented a literature review on this topic, comparing 77 papers and classifying them based on smart building applications, adopted metrics and algorithms. Figure 2.10 displays the applications adopted in smart buildings, relating them to the TL classifications and techniques discussed previously.
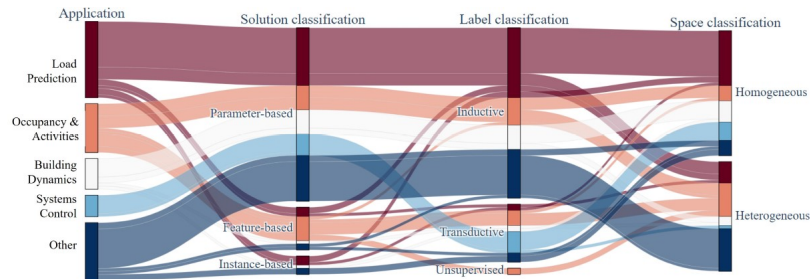
Fig. 2.10: Sankey diagram based on TL applications, techniques and categories [7].

Chapter 3

Case study

3.1 Case study description

This case study concerns a medium-size reference office building (shown in figure 3.1), on which thirty-one years were simulated through Open Studio and Energy Plus and saved in a compressed hierarchical data format (HDF5). The available features regard system-level and end-use level information thanks to the *Building Energy Management System* (BEMS), which provides system-level sub-metering of electricity consumptions and zone-level indoor environmental measurements. Simulations were carried out with the following assumptions:

- physics-based building thermal simulations are based on a detailed building thermal zoning;

- MELs and HVACs schedules were used to represent stochastic occupancy profiles, based on space level and thermal zone;

- all data exploited and outcoming from simulations were saved in an HDF file format, suitable to reduce disk size requirements and store models, climate files, metadata and time-series data.

The building model used for the project is a medium-size office building of three floors with a total floor areas of 4890 square meters. This building is one of the commercial building models developed by the U.S. Department of Energy (DOE), representing 70% of U.S. commercial buildings. As shown in figure 3.1, this office is composed by 12 space types: open and enclosed office rooms, conference room, classroom, dining area, lobby, corridor, stair, storage, restroom, plenum, and mechanical room.
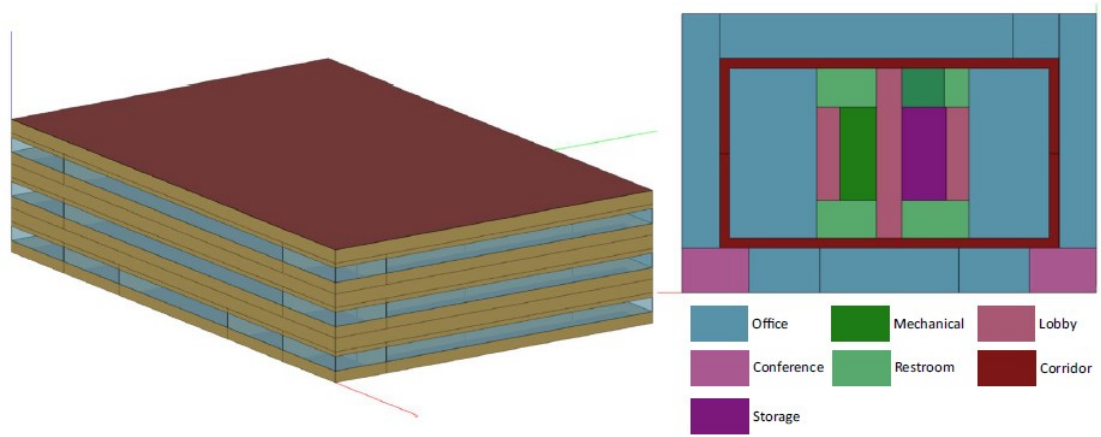
Fig. 3.1: Building geometry and thermal zones [8].

Regarding the conditioning system, the building is served by three Air Handling Units (AHUs) with Variable Air Volume (VAV), one per floor. Furthermore, the AHUs are equipped with air cooled direct expansion cooling coil and gas heating coil; each zone is served by VAV terminal unit with reheat coil. The creation of the whole data set follow the workflow in figure 3.2.
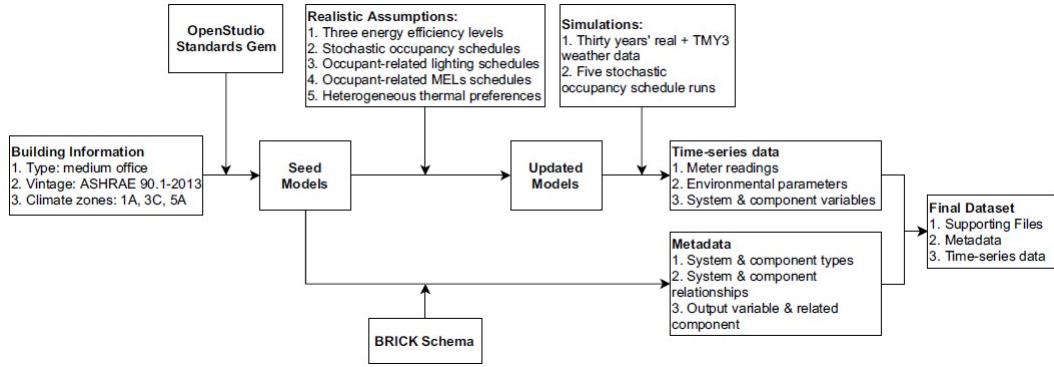
Fig. 3.2: Workflow of data generation [8].

Starting from building information input (building type and climate zone), the building energy modeling software Open Studio and particularly Open Studio Standard Gem (a specific software library), were used to carry out the simulations. The seed model was created and then modified changing building envelop properties, thermostat set-point, MELs and HVAC system efficiency, in order to generate three different building efficiency levels and represent real building operations. To simulate the effect of different climate conditions, three climate files were considered, corresponding to three locations: San Francisco (3C), Miami (1A) and Chicago (5A). Mean temperature and humidity trends of these locations are shown in figure 3.3.
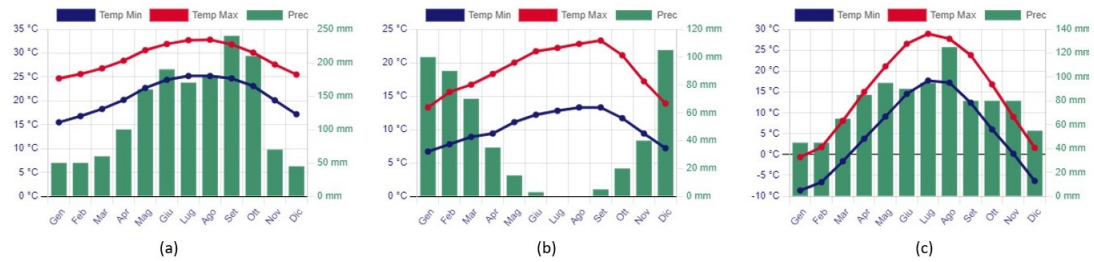
Fig. 3.3: Mean air temperature and humidity of Miami (a), San Francisco (b) and Chicago (c).

Power consumption for lighting/MELs/occupancy density and efficiency levels are shown below in tables 3.2 and 3.2.

Table 3.1: Lighting, MELs and Occupancy of the main space types [8].

Space Type	Lighting power density (W/m2)	MELs power density (W/m2)	Occupancy density (m2/p.)
Open office	13.2	12.9	12.2
Enclosed office	14.9	11.7	20
Conference room	16,5	13.5	2.5
Classroom	16.7	12.5	2.7
Corridor	8.9	3.9	n.a.
Stair	9.3	n.a.	n.a.
Dining room	8.7	13.4	9.3
Lobby	12.1	3.6	9.3
Mechanical room	12.8	3.6	n.a.

Table 3.2: Systems efficiency levels [8].

Efficiency Level	Low	Standard (ASHRAE 90.1–2013)	High
COP of AHU	1,8	2,4	3
Water heater thermal efficiency	46,7%	62,3%	77,9%
Gas burner efficiency	48,0%	64,0%	80,0%
VAV reheat coil efficiency	60,0%	80,0%	95,0%
Fan total efficiency	36,3%	48,4%	60,5%
Pump motor efficiency	18,0%	24,0%	30,0%
Envelope thermal resistance	0.75 standard level	varies by climate	1.25 standard Level

Moreover, five stochastic occupancy profiles were created to highlight the differences in user preferences due to their age, culture, gender and corresponding lighting, MELs and HVAC operations. An example of comparison between the original profiles and the updated ones are shown in figure 3.4.
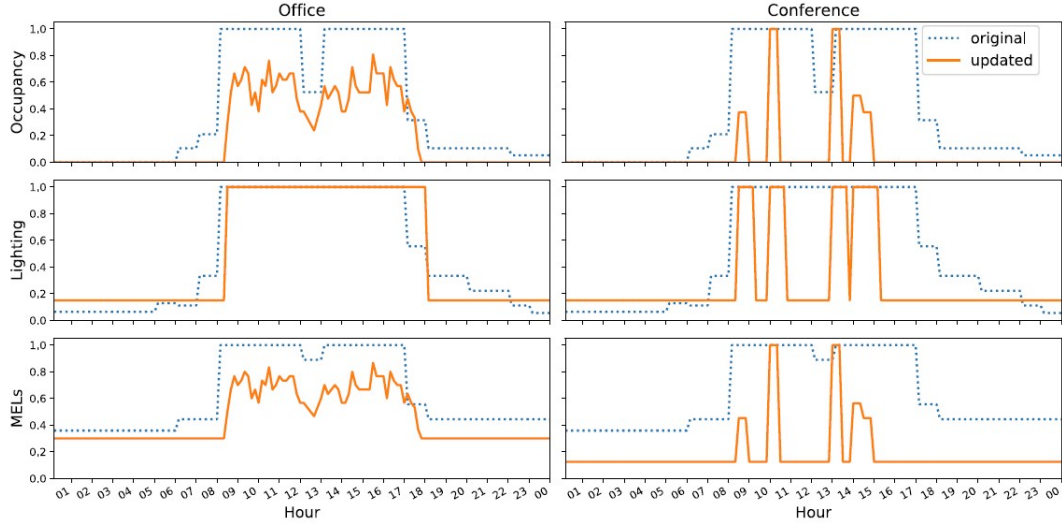
Fig. 3.4: Occupancy, lighting and MELs profiles between office and conference rooms [8].

3.2 Simulations outcomes

Each configuration was then simulated with thirty years of historical weather plus one Typical Meteorological Year (TMY3) weather data. Each simulation provides a time-serie and all of them were saved in a unique Hierarchical Data Format (HDF5) file, to reduce memory requirements and improve file reading and writing efficiency. To sum up, 3 (locations) x 3 (efficiency levels) x 5 (occupancy/MELs, lighting profiles) x 31 (weather files) = 1395 models were obtained. Each model represent time-series with a time-step of 10 minutes and 35 output variables, shown in table 3.3 with the corresponding variable type, dimension and size.

Table 3.3: Simulations output variables [8].

Name	Variable Type	Dimension (rows columns)	Size (MB)
Air System Outdoor Air Economizer Status	System Variable	525.603	3
Cooling Electricity	Energy	525601	2
Electricity Facility	Energy	525601	2
Electricity HVAC	Energy	525601	2
Exterior Lights Electricity	Energy	525601	2
Fan Air Mass Flow Rate	System Variable	525603	3
Fan Electric Power	Power	525603	3
Fans Electricity	Energy	525601	2
Gas Facility	Energy	525601	2
Gas HVAC	Energy	525601	2
Heating Electricity	Energy	525601	2
Interior Equipment Electricity	Energy	525601	2
Interior Lights Electricity	Energy	525601	2
Pump Electric Power	Power	525601	2
Pump Mass Flow Rate	System Variable	525601	2
Pumps Electricity	Energy	525601	2
Site Day Type Index	Other Variable	525601	2
Site Horizontal Infrared Radiation Rate per Area	Other Variable	525601	2
Site Outdoor Air Dewpoint Temperature	Other Variable	525601	2
Site Outdoor Air Drybulb Temperature	Other Variable	525601	2
Site Outdoor Air Relative Humidity	Other Variable	525601	2
Site Outdoor Air Wetbulb Temperature	Other Variable	525601	2
System Node Mass Flow Rate	System Variable	52560377	153
System Node Pressure	System Variable	52560377	153
System Node Relative Humidity	System Variable	52560377	153
System Node Temperature	System Variable	52560377	153
Zone Air Relative Humidity	Zone Variable	5256068	29
Zone Air Terminal VAV Damper Position	Zone Variable	5.256065	28
Zone Electric Equipment Electric Power	Power	5256047	20
Zone Lights Electric Power	Power	5256065	28
Zone Mean Air Temperature	Zone Variable	5256068	29
Zone Mechanical Ventilation Mass Flow Rate	Zone Variable	5256065	28
Zone People Occupant Count	Zone Variable	5256028	13
Zone Thermostat Cooling Setpoint Temperature	Zone Variable	5256068	29
Zone Thermostat Heating Setpoint Temperature	Zone Variable	5256068	29

From results, it is noted how the energy consumption changes base on efficiency levels, weather and day of the week (weekend or not). The

relationship between these variables are shown in figure 3.5.
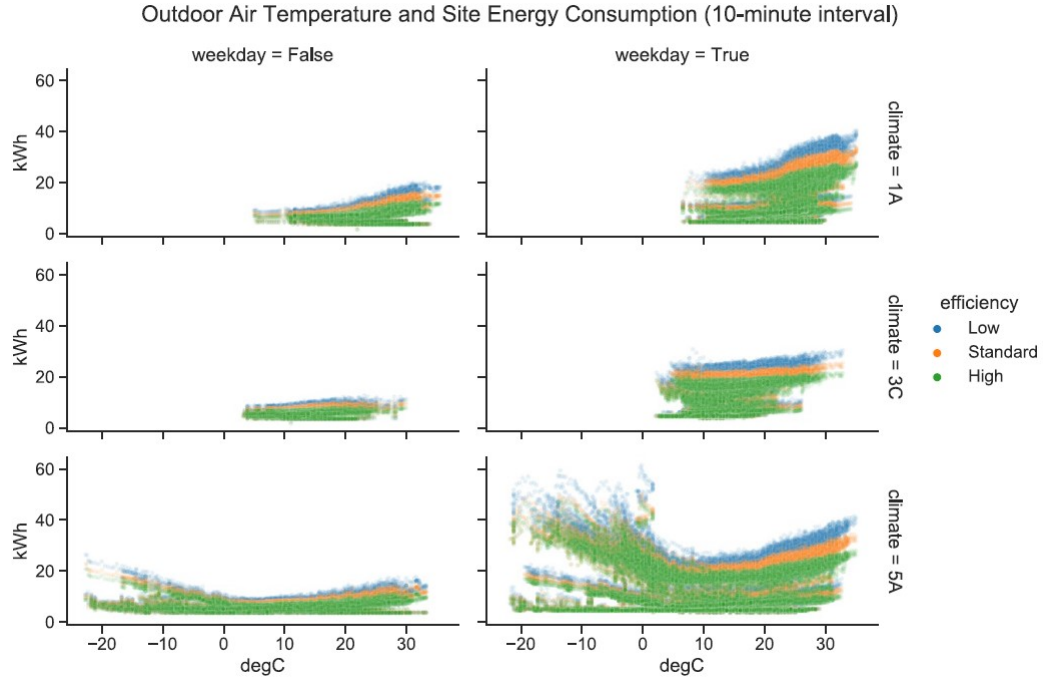
Fig. 3.5: Relationship between energy consumption, efficiency levels and weather [8].

As expected, energy consumption increases respectively with the decrease of efficiency, and it is higher during the weekdays with respect to the weekend. Consumption trend is approximately constant in climate 3C and varied in climate 5A, because of the higher temperature variation between seasons in Chicago.

At the end of simulations, all csv time series obtained were converted and saved in an Hierarchical Data Format (HDF5), that supports an unlimited variety of data types, and is designed for flexible and efficient I/O and for high volume and complex data.

Chapter 4

Methodology

In this chapter will be exposed the steps involved in this study. Starting from a classification based on the information level of each variable outcomes from EnergyPlus simulations, a selection of features suitable for an accurate indoor air temperature prediction were done. Two neural networks have been developed and after the identification of their principal hyperparameters, a tuning of these have been applied through an optimization library called OPTUNA [27]. After an analysis of NNs' metrics, the NN model which allowed the best metrics has been taken into account for the next steps. The last two sections will concern the description of all cases deployed, machine learning techniques applied and the metrics adopted to evaluate the models accuracy. Figure 4.1 sums up all these steps.
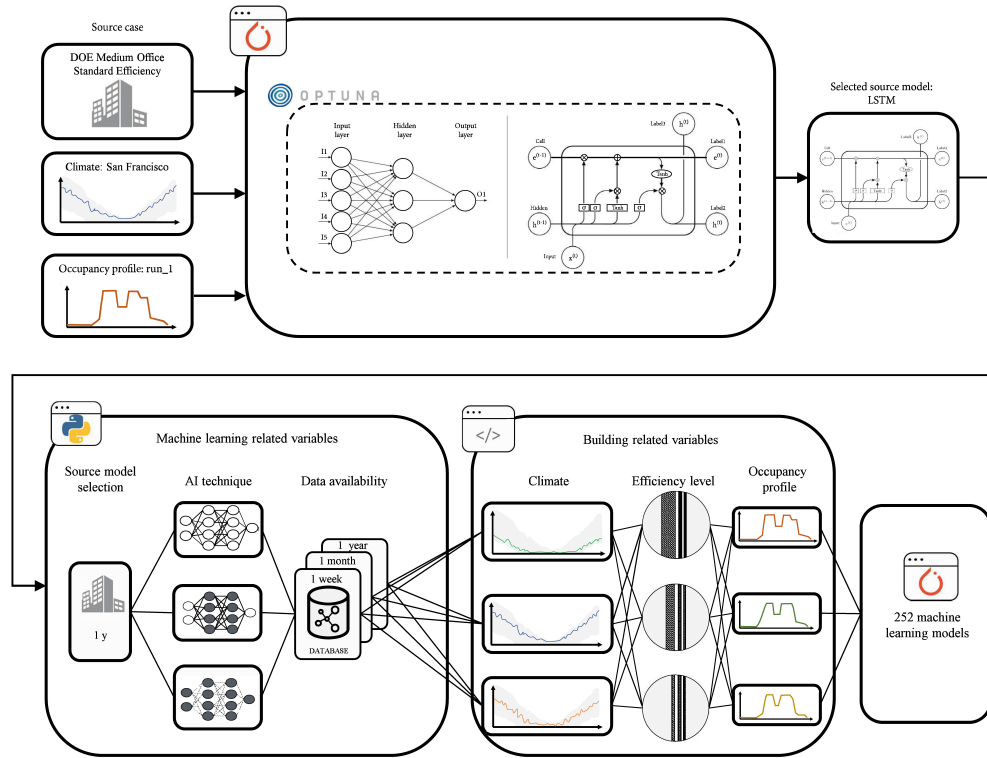
Fig. 4.1: Methodology adopted in the thesis.

Firstly a source model will be selected and this will be exploited to testing the two NN model types and select the better one. Next step concerns the quantification of zone orientation influences, analyzing three different zones with the same boundary conditions. Successively, to evaluate the goodness of prediction in respect to the other features, all of these will be crossed in order to create nearly 30 different cases based on the same zone but different boundary conditions, as efficiency level, occupancy profile as well as the climate file.

4.1   Input features selection

Simulation outcomes shown in table 3.3 don't provide the same information
level for all variables. It is possible to distinguish three information level as
following in table 4.1.

Table 4.1: Simulations outcomes information levels.

Building level	AHU level	Zone level
Cooling Electricity [J]	Air System Outdoor Air Economizer Status [-]	System Node Mass Flow Rate [kg/s]
Electricity Facility [J]	Fan Air Mass Flow Rate [kg/s]	System Node Pressure [Pa]
Electricity HVAC [J]	Fan Electric Power [W]	System Node Relative Humidity [%]
Exterior Lights Electricity [J]		System Node Temperature [°C]
Fans Electricity [J]		Zone Air Relative Humidity [%]
Gas Facility [J]		Zone Air Terminal VAV Damper Position [-]
Gas HVAC [J]		Zone Electric Equipment Electric Power [W]
Heating Electricity [J]		Zone Lights Electric Power [W]
Interior Equipment Electricity [J]		Zone Mean Air Temperature [°C]
Interior Lights Electricity [J]		Zone Mechanical Ventilation Mass FlowRate [kg/s]
Pump Electric Power [W]		Zone People Occupant Count [-]
Pump Mass Flow Rate [kg/s]		Zone Thermostat Cooling Set-point Temperature [°C]
Pumps Electricity [J]		Zone Thermostat Heating Set-point Temperature [°C]
Site Day Type Index [-]		

In addiction to these, outdoor variables are summary in table 4.2.

Table 4.2: Outdoor simulations outcomes.

Outdoor simulation outcomes
Site Horizontal Infrared Radiation Rate per Area [W/m2
Site Outdoor Air Dewpoint Temperature [°C]
Site Outdoor Air Drybulb Temperature [°C]
Site Outdoor Air Relative Humidity [%]
Site Outdoor Air Wetbulb Temperature [°C]

Not all features listed in table 4.1 and 4.2 were selected for the training phase. The selection process depends on the accuracy level with which you want to describe the building model. In this case a zone level was selected for the model training and features take into account indoor, outdoor and conditioning system properties, as listed in table 4.3.

Table 4.3: Training model features.

Selected training features
Zone Thermostat Cooling Set-point Temperature [°C]
Zone Thermostat Heating Set-point Temperature [°C]
Zone People Occupant Count [-]
Zone Mechanical Ventilation Mass Flow Rate [kg/s]
Zone Mean Air Temperature [°C]
Site Day Type Index [-]
Site Horizontal Infrared Radiation Rate per Area [W/m2]
Site Outdoor Air Wetbulb Temperature [°C]

4.2   Neural networks design

As anticipated in the previous chapters, in this study two neural networks are compared: a MLP and a LSTM. NN models developed in this study were trained on 8 h of medium office building features data, with a time step of 10 minutes, with the goal to predict indoor air temperature evolution for the next hour. Thus, for each prediction 6 values are obtained and compared with the real ones during the training phase, to update the model accuracy. Each of these two NN has different hyperparameters that aim learning process optimization; some of these are in common as shown in table 4.4, .

Table 4.4: NN models hyperparameters.

LSTM	MLP
Number of LSTM layers	Input features number of each layer
Number of neurons for each layer	Output features number of each layer
Batch size	
Learning rate	
Epochs	

4.3   Hyperparameters tuning

The first step concerns the exploitation of an optimization library called OPTUNA [27], with which is possible to fit a range for each model hyperparamenter and run an arbitrary number of trials. Each trial consist on a simulation with a specific value for each hyperparameter, included in the range fitted previously, aiming the optimization of one or more metrics (in this case the MAPE was selected). For both the NNs, 6 optuna simulations were run. The first five simulations needed to understand how performance change respect to hyperparameters values; thus, they allow to restrict the field freedom degrees. Once this is done, the last simulation provides the final optimal hyperparameters values for each neural network. The source model selected concerned one conference room of the ground floor, with a standard efficiency and the first occupancy profile. NN models were trained on 1 year of data and tested for another year, which is specifically a Time Meteorological Year (TMY): a set of meteorological data with data values for every hour in a year for a given geographical location. The data are selected from hourly data in a longer time period (normally 10 years or more). For each month of the year, data have been selected from the year that was considered most "typical" for that month. At the end of this step, the optimal models hyperparameters obtained are listed in tables 4.5 and 4.6.

Table 4.5: LSTM model optimal hyperparameters.

LSTM	
Number of layers	3
Number of neurons per layer	175
Epochs	90
Learning rate	0.0077
Batch size	900
MAPE	0.535

Table 4.6: MLP model optimal hyperparameters.

MLP	
Number of outputs from the layer 1	100
Number of outputs from the layer 2	70
Number of outputs from the layer 3	70
Number of outputs from the layer 4	10
Epochs	120
Learning rate	0.00757
Batch size	900
MAPE	1.096

As noted in tables 4.5 and 4.6, the LSTM provides a better accuracy, so it will be the architecture used for transfer learning applications. The two models are displayed in figure 4.2 and figure 4.3.
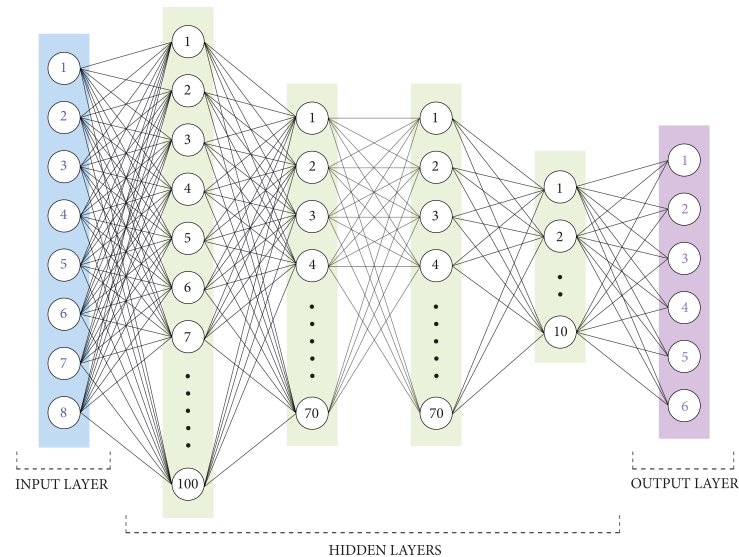
Fig. 4.2: Case study MLP structure.
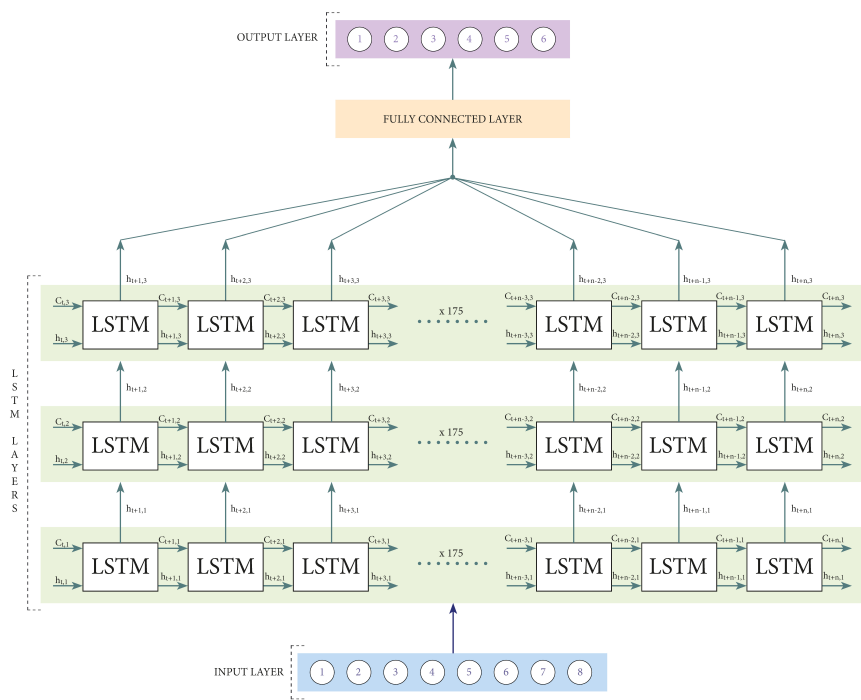
Fig. 4.3: Case study LSTM structure.

4.4 Transfer learning scenario

The study focuses on the influence of specific features to analyze the effectiveness of TL for building thermal dynamic models. In particular, the following features were deeply analyzed:

- 4 different zones: a conference room at the bottom floor, a conference room and an enclosed office at the middle floor and an open office at the third floor;

- all climate files: 1A (Miami), 3C (San Francisco), 5A (Chicago);

- all efficiency levels: low, standard and high;

- 3 occupancy profiles: run 1, run 2, run 3.

To understand how much the zone, the climate, the occupancy profiles (MELs and lighting consequently) and the efficiency level affect the performance of the model, a combination between all variables listed above was done, by creating nearly 30 cases. For each case obtained, three different techniques were applied and compared: machine learning (ML), feature extraction (TL-FE) and weights initialization (TL-WI), each one tested to one week, one month and one year, obtaining more than 250 simulations. Cases will be identified with the format <zone><climate file><efficiency><occupancy profile>. Firstly, 3 zones, different from the source one, were compared testing them on one month of target data. In table 4.7, are shown simulations run more specifically:

For the next simulations, the model will be tested on one week, one month and one year. Solely, when one year of data is available, machine learning is used instead of transfer learning, because there are enough data to training a model with good performance; however in this study TL was also applied on one year, as an ideal case. Thus, maintaining locked the zone, changing all others features, combining every possible crossing case for 3 different

Table 4.7: Simulations on three different building zones.

Zone	Climate	Efficiency	Occupancy profile	Technique	Training time	Testing time	Epochs
CONFROOM MID 2	3C	Standard	run 1	ML	1m	1m	90
CONFROOM MID 2	3C	Standard	run 1	FE	1y	1m	80
CONFROOM MID 2	3C	Standard	run 1	WI	1y	1m	80
ENCLOSEDOFFICE BOT 2	3C	Standard	run 1	ML	1m	1m	90
ENCLOSEDOFFICE BOT 2	3C	Standard	run 1	FE	1y	1m	80
ENCLOSEDOFFICE BOT 2	3C	Standard	run 1	WI	1y	1m	80
OPENOFFICE BOT 3	3C	Standard	run 1	ML	1m	1m	90
OPENOFFICE BOT 3	3C	Standard	run 1	FE	1y	1m	80
OPENOFFICE BOT 3	3C	Standard	run 1	WI	1y	1m	80

time period and 3 technique applied, 9 (shown in table 4.8) runs for each case were obtained, to examine the combining effect of each feature.

Table 4.8: Simulations run for each case, based on technique exploited, training and testing periods.

Technique	Training period	Testing period
ML	1y	1y
ML	1m	1m
ML	1w	1w
FE	1y	1y
WI	1y	1m
FE	1y	1w
WI	1y	1y
FE	1y	1m
WI	1y	1w

The wide amount of simulations run are listed in table 1 in Appendix A.

4.5 Evaluation metrics

To evaluate the effectiveness of ML and TL and models performance, several metrics have been identified, including:

- *Mean absolute percentage error* (MAPE): a lower result implies better performance and it provides the degrees of the inaccuracy in percentage

terms:

$$MAPE = \frac{100}{n} \sum_{t=1}^{n} \left| \frac{y_{real} - y_{pred}}{y_{real}} \right| \tag{4.1}$$

- *Mean absolute error* (MAE): is a an usual statistic for assessing forecast accuracy:

$$MAE = \frac{\sum_{i=1}^{n} |y_{pred} - y_{real}|}{n} = \frac{\sum_{i=1}^{n} |e_i|}{n} \tag{4.2}$$

- *Mean squared error* (MSE): It penalizes greater error values and can be higher than MAE due outliers:

$$MSE = \frac{\sum_{i=1}^{n} (y_{real} - y_{pred})^2}{n} \tag{4.3}$$

- *Jumpstart*: the difference amount between the starting performance value between ML and TL techniques.

- *Time to threshold*: time needs to reach a certain accuracy in the target task.

- *Asymptotic performance*: the difference between the last performance value, at the end of the simulation.

MAPE, MAE and MSE have been calculated either for each time step and as total mean of these. Instead, last three metrics are illustrated in figure 4.4.
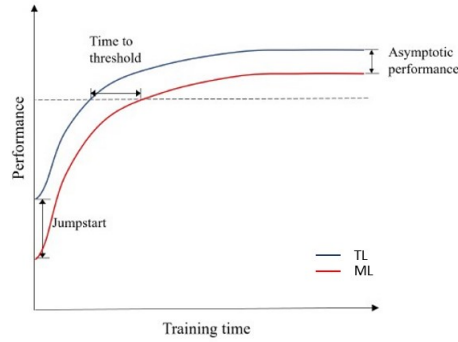
Fig. 4.4: Jumpstart, time to threshold and asymptotic performance metrics [7].

These metrics need to answer at some questions like:

- what is the error quantified between real and predicted values?

- how much is the computational time required to make the model able to predict indoor air temperature with a good accuracy?

- how much TL started and final performance are better than ML ones?

In chapter 5, results obtained from all simulations introduced previously will be shown and analyzed.

Chapter 5

Results

The chapter studies in detail the influences of the different features on prediction accuracy, exploiting three techniques to carry on the simulations: simple machine learning and two transfer learning solutions (features extraction and weights initialization) . Firstly the zone variable is examined, comparing three zones, different from the source one, but with the same boundary conditions. Once learned how much the zone affects the goodness of the prediction, other features are taken into account. Thus, considering the same zone of the source one, next examination regards the efficiency level, occupancy profile, weather file and training/testing influence. Lastly, a classification of all features are made, to quantify what variables have the major impact on prediction issue.

5.1 Zone analysis

The three zones selected for this analysis are a conference room and an enclosed office on the middle floor, and a open office at the top floor; all of these have a different orientation, which is the examined characteristic. The zone are respectively named as <CONFROOM_MID_2>, <OPENOFFICE_BOT_3> and <ENCLOSEDOFFICE_BOT_2>. At each floor are

presented more zones with the same function and it's the reason why at the end of each format there is a number. As described in chapter 4, to allow a good prediction accuracy and teach the model to understand features relationship, a training phase is necessary. During this phase, at each epoch, weights of all neurons are tuned through the calculation of a loss function; in this study the MSE loss was selected. Following figures display the loss function trend for each zone and technique.
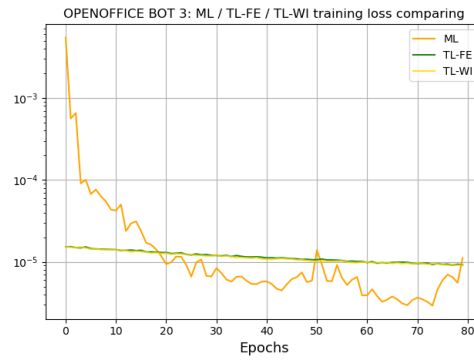
Fig. 5.1: MSE loss function trend of bottom floor open room.
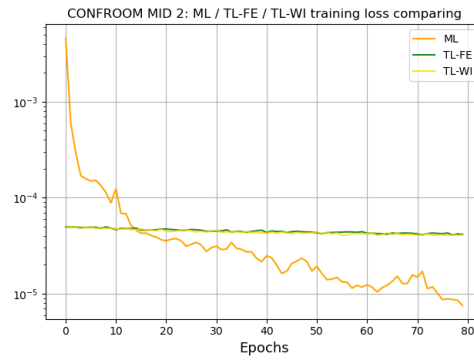
Fig. 5.2: MSE loss function trend of middle floor conference room.
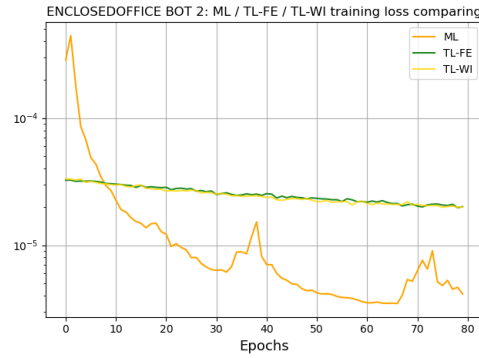
Fig. 5.3: MSE loss function trend of bottom floor enclosed room.

From figures above it's possible to notice some observations. First of all, ML loss function is deeper respect to TL_FE and TL_WI. This happens because during ML training phase the model learns features relationship for the first time, and when TL is executed, the first training phase has been applied yet and the learning rate is reduced, so the slope is lower. Moreover, TL_FE and TL_WI loss trends are very similar. Regarding the testing phase, a MAE and MSE comparison for each prediction step could give an evidence of the better performance of TL methods respect to the simple ML one. This benchmarking is shown in the following figures for each zone.
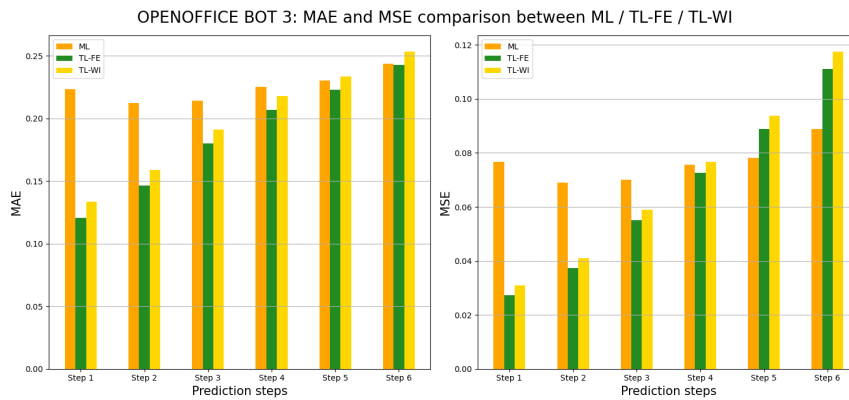
Fig. 5.4: Testing phase MAE and MSE for bottom floor open room.
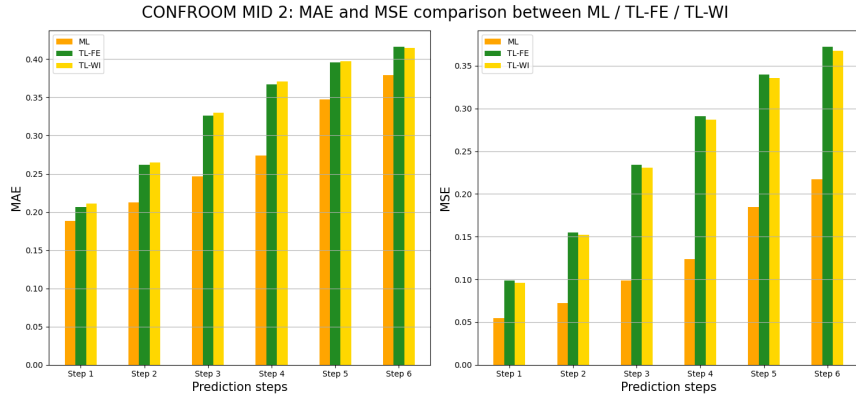
Fig. 5.5: Testing phase MAE and MSE for middle floor conference room.
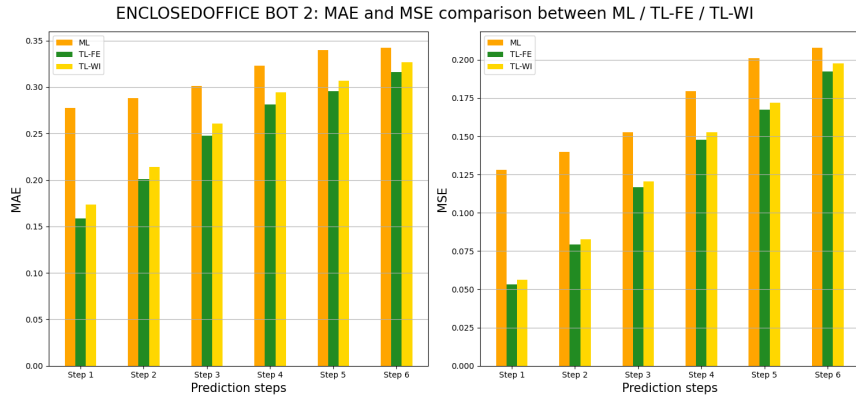
Fig. 5.6: Testing phase MAE and MSE for bottom floor enclosed room.

Figures 5.5, 5.4 and 5.6 highlight that, as expected, both metrics increase proportionally with the time horizon in all cases; moreover the major gap between ML and TL techniques are higher for the first steps. Differently for the two offices, for the conference room ML has better performance than TL. This could be explained considering that the ML learning have been just applied on the same zone type, and an further training could bring to an overfitting of the model.

5.2   Technique analysis

This section pays a particular attention to the difference between the model accuracy based on the technique applied. Considering the whole data set, without distinguishing training and testing periods, system efficiencies as well as the occupancy profiles, analyzing the density distribution of the mean MAE of the simulations run, figure 5.7 is obtained.
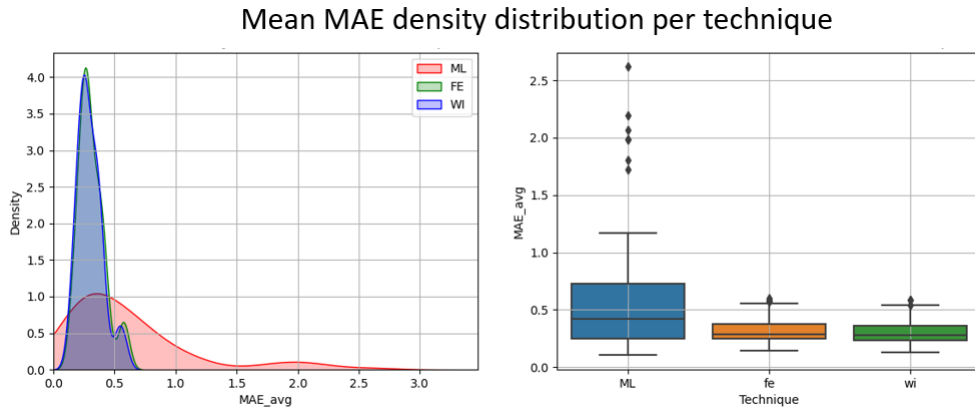
Fig. 5.7: Mean MAE density distribution per technique.

This figure highlights the extension of ML technique error, which has a maximum nearly to 3 °C, opposite to the others techniques application results, that are totally condensed in a range between 0 °C and 0.6 °C. It is visible that more than 50% of ML simulations have a grower MAE respect to that obtained with both TL methods.

5.3   Training period analysis

Another additional analysis concerns the availability of data exploited to train the model. In this study tree training period were taken into account: one week, one month and one year. Thus, for each prediction step and training period, metrics resulted are displayed in figure 5.8, 5.9 and 5.10.
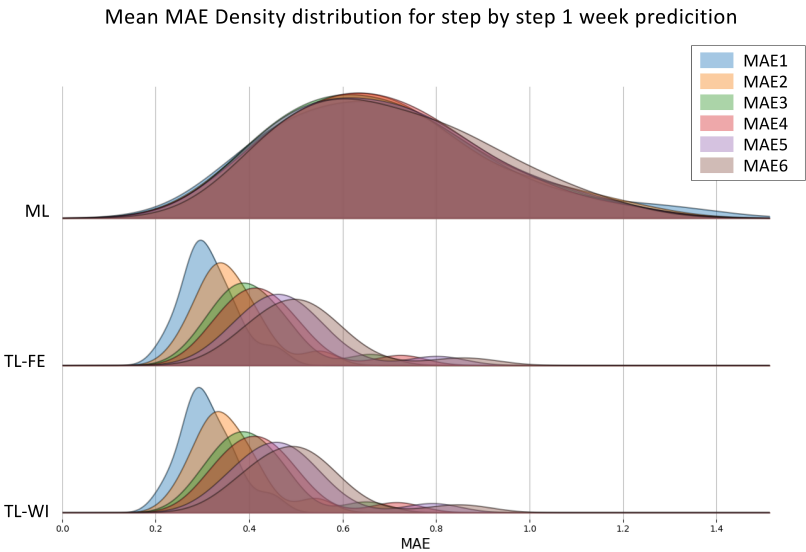
Fig. 5.8: Mean MAE density distribution per technique and a training period of 1 week.
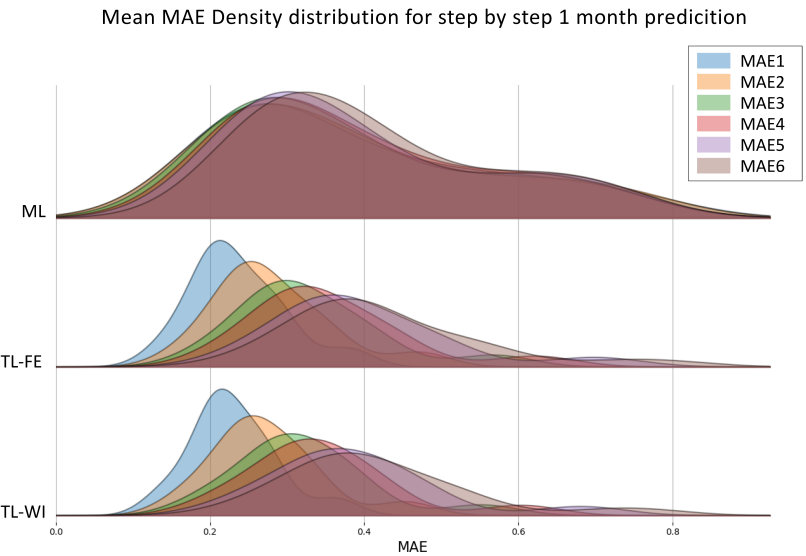
Fig. 5.9: Mean MAE density distribution per technique and training period of 1 month.
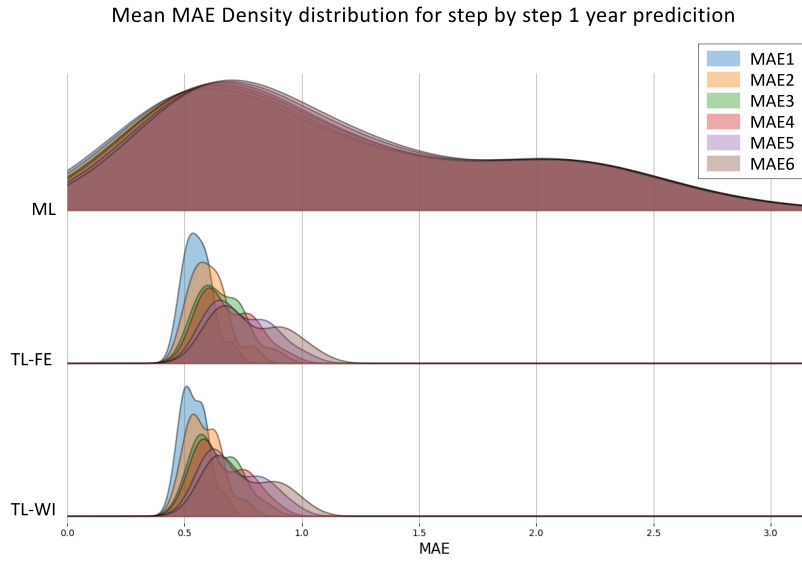
Fig. 5.10: Mean MAE density distribution per technique and training period of

1 year.

These figures confirm that the models performance get worse with the rise of the prediction horizon and results provides a lower accuracy for ML respect to the TL one, whatever is the training period and consequently the data availability. Moreover, it is evident that, a model tuned on one month has the best performance; while, on the other side, weekly training period provides the worst accuracy. This is explainable considering that one year of data includes a wider temperature variation, especially for more critical climate as Chicago (5A); this factor could deceive the model that couldn't understand features relationship; thus, training the model on one month at a time provides a tuning on a more uniform temperature trend and, consequently, better prediction performance.

5.4   Climate analysis

The climate proved to be among the most interesting factor to be analyzed. In figure 5.11 is displayed the mean MAE distribution, based on climate

file, technique and testing period. First of all, paying attention to the scale
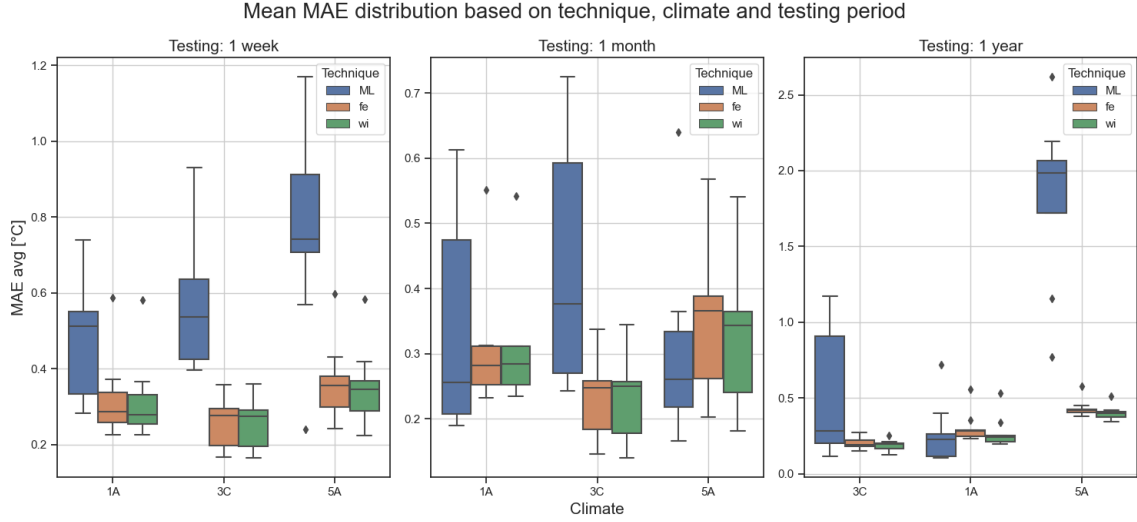
Fig. 5.11: Mean MAE distribution based on technique, climate and testing period.

of each axis, the results put on view that a testing period of one month provides the lowest prediction error. Additionally, the model struggles to predict the indoor air temperature with the 5A climate type, which has the greatest temperature range from winter to summer season. Another evidence of figure 5.11 is that ML is not always the worse method respect to TL alternatives, like in case of climate 5A/monthly testing and climate 1A/yearly testing; this event is called *Negative Transfer*. Furthermore, despite FE and WI accuracy are similar, the WI method provides the higher performance in all cases, probably because a tuning of all layers help the model to adapt better its weights to the target data.

5.5 Statistical evaluations

In this chapter a statistical analysis of all features affecting model performance is presented. First of all, in figure 5.12, the *Asymptotic performance* (also called *Performance improvement ratio*) is displayed for all cases imple-

mented in this thesis. As shown in section 4.5, the asymptotic performance is
the gap between the ML and TL testing accuracy value of the last simulation
epoch.
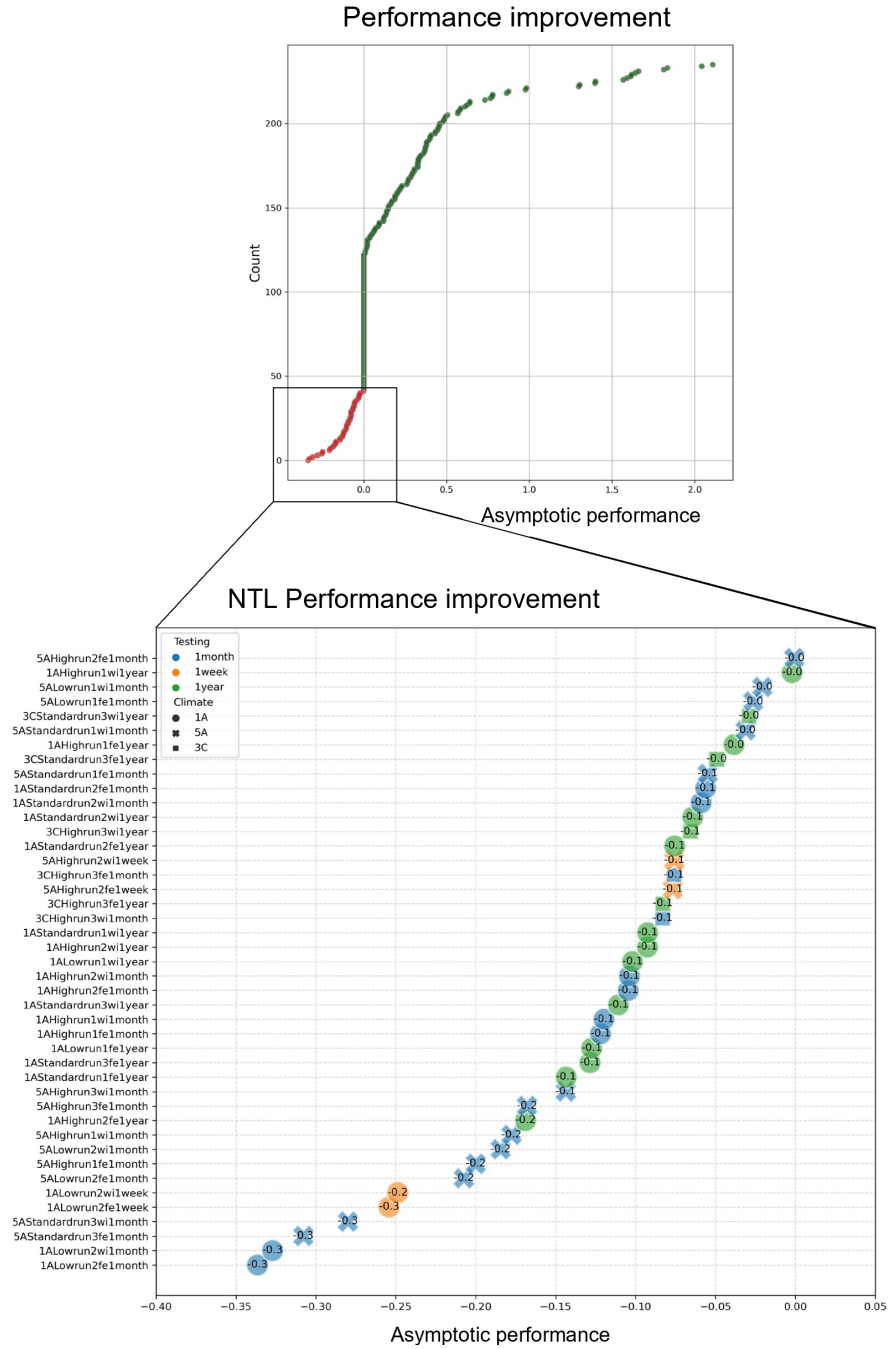
Fig. 5.12: Negative transfer learning analysis

In the upper plot it is visible that more than 80% of TL applications metrics overcome ML ones, while for nearly 15% of cases, Negative Transfer Learning (NTL) occurs. This event is focused in the lower plot. It is noted that the majority of NTL happens with monthly and yearly data availability with different climates; in particular, climate 5A and 1A occurs more. The occurrence of NTL doesn't means that TL get worse, rather that both ML and TL reach high accuracy and perform similarly when these two data amounts are available. Both climates 5A and 1A are different respect to the source one (3C), and they occurs more when compare respectively with monthly and yearly availability. Thus, climate variable is the more affecting feature, and ML reaches good performance with monthly availability. So, if the target building dynamic is similar to the source one, TL is not the only efficient solution. Regarding the occupancy profiles, results indicate an uniform occurrence of all that and no one is particularly distinguished.

Next step concerns the development of regression tree to characterize the feature importance with different data availability. This instrument is created using a method called binary recursive partitioning, which is an iterative procedure that divides data into partitions or branches, then separates each partition into smaller groups as the algorithm progresses up each branch. The Training Set's records are initially sorted into the same division. The method then divides the data into the first two divisions or branches, taking use of every potential binary split on each field. The split that minimizes the sum of the squared deviations in the two independent partitions is chosen by the algorithm. Each of the new branches is then divided according to this rule. This procedure is repeated until each node meets the minimum node size chosen by the user or automatically and becomes a terminal node, called *leaf node*. In this case the data exploited are the climate file, the efficiency level, the occupancy profile, the technique method and testing period; while as output the resulting MAE is given.

The tree displayed in figure 5.13 was implemented on the whole data set.
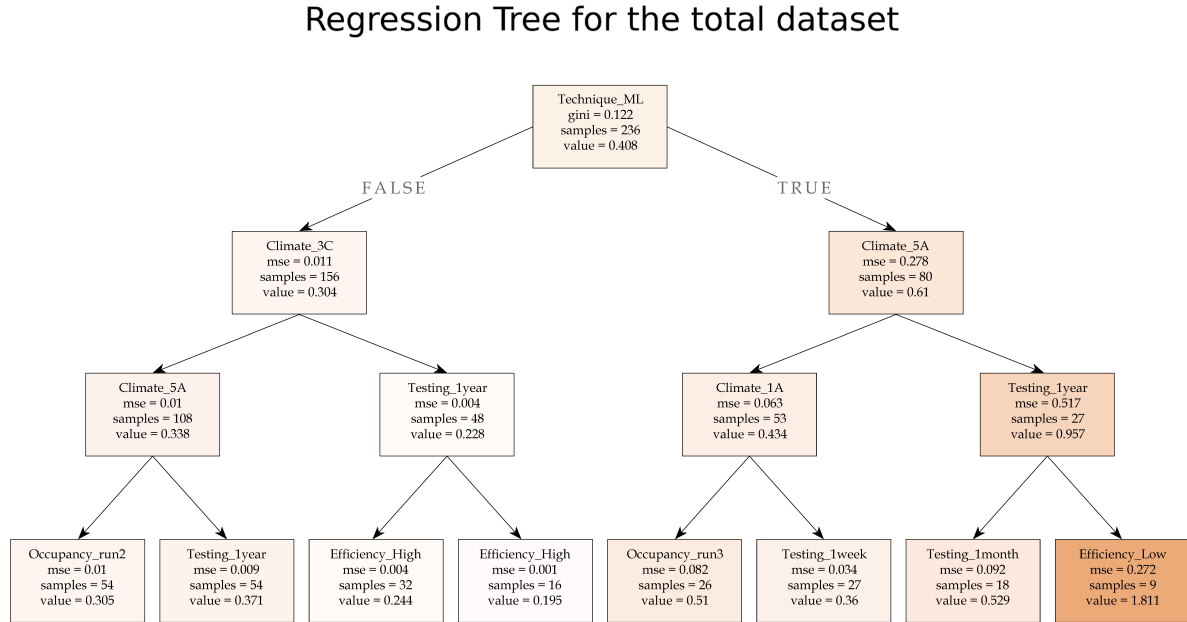
Fig. 5.13: Regression Tree for the total data set

This regression tree demonstrate that, in order of importance, metrics are affected by technique method, climate type, testing period, occupancy profile and efficiency level. From these results 3 metric ranges was extrapolated: $[0, 0.3), [0.3, 0.7), [0.7, 3]$. The next step concerns the creation of classification trees, distinguishing the three testing periods. Before do it, the intervals listed previously were converted in prediction performance classes:

- $[0, 0.3)$: High performance;

- $[0.3, 0.7)$: Medium performance;

- $[0.7, 3]$: Low performance.

The classification trees were stopped to the third deph level; results obtanied are shown below in figure 5.14, 5.15, 5.16:
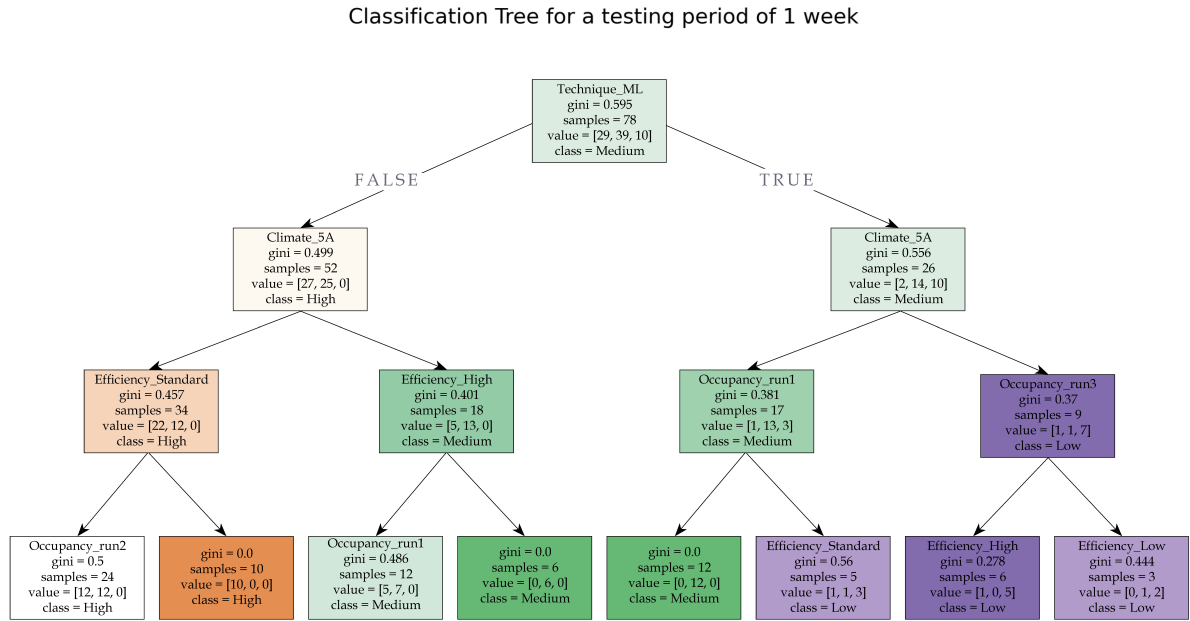
Fig. 5.14: Classification Tree for a testing period of one week.
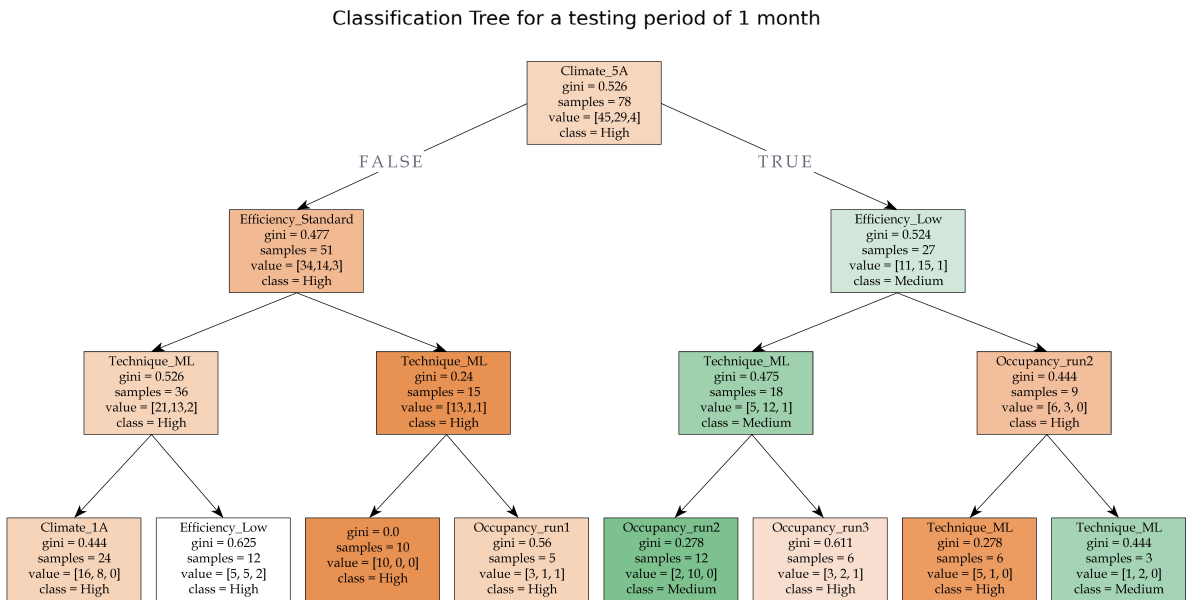
Fig. 5.15: Classification Tree for a testing period of one month.
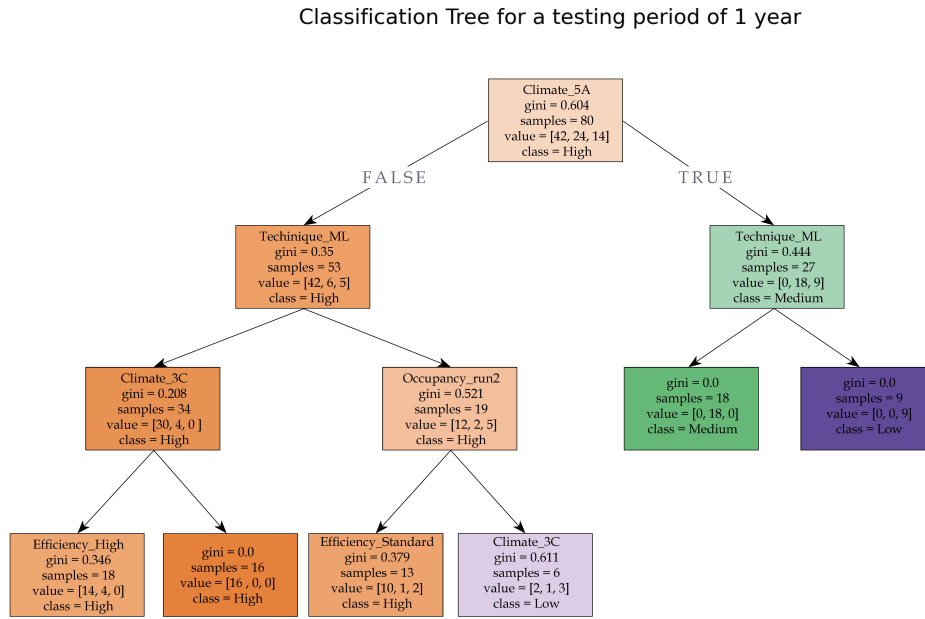
Fig. 5.16: Classification Tree for a testing period of one year.

Taking a look at these trees, the first visible consideration is the absence of the Low class in the monthly tree; this reflects results previously obtained, evaluating the monthly testing period as the better one for reaching higher performance; on the other hand the weekly testing period aims the worse accuracy because of the limited data availability. In all trees, technique method, climate file and efficiency profile result to be the best discriminant features. Another reflection regards the fact that every time happens the combination between climate 5A and ML method on the upper nodes, low performance are obtained at the leaf nodes. This consequence reflects the negative transfer results explained before. The gap between TL-FE and TL-WI resulting classes are placed on the same level in all trees and, every time they occurs, higher accuracy are provided as verified in the previously analysis. Regarding the occupancy profiles, it hasn't a primary role on the classes classification as noted also in the regression tree. As anticipated in the chapter 3, the occupancy profiles were chosen arbitrarily and related to them also MELs and lighting profiles. In figure 5.17 a day type occupancy

is shown and it's noted that occupancy 1 and 3 are more similar.
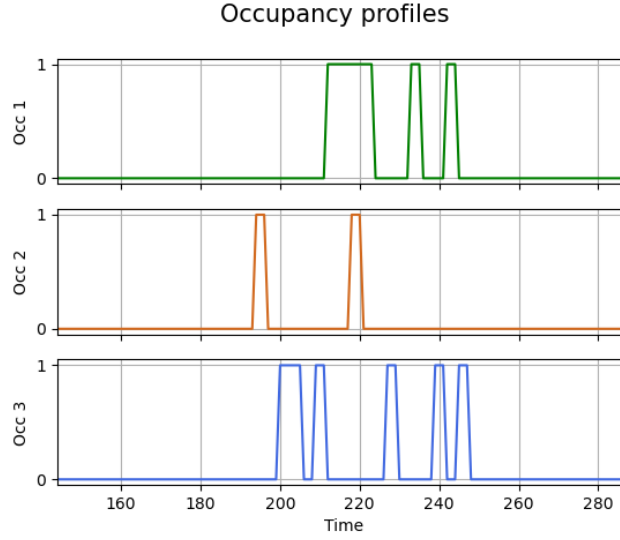
Fig. 5.17: Occupancy profiles of a day type.

To confirm all evidences extrapolated from results and graphs shown until now, in figure 5.18 the real indoor air temperature evolution respect to that obtained through ML, TL-FE and TL-WI is displayed, in both positive and negative transfer learning cases.
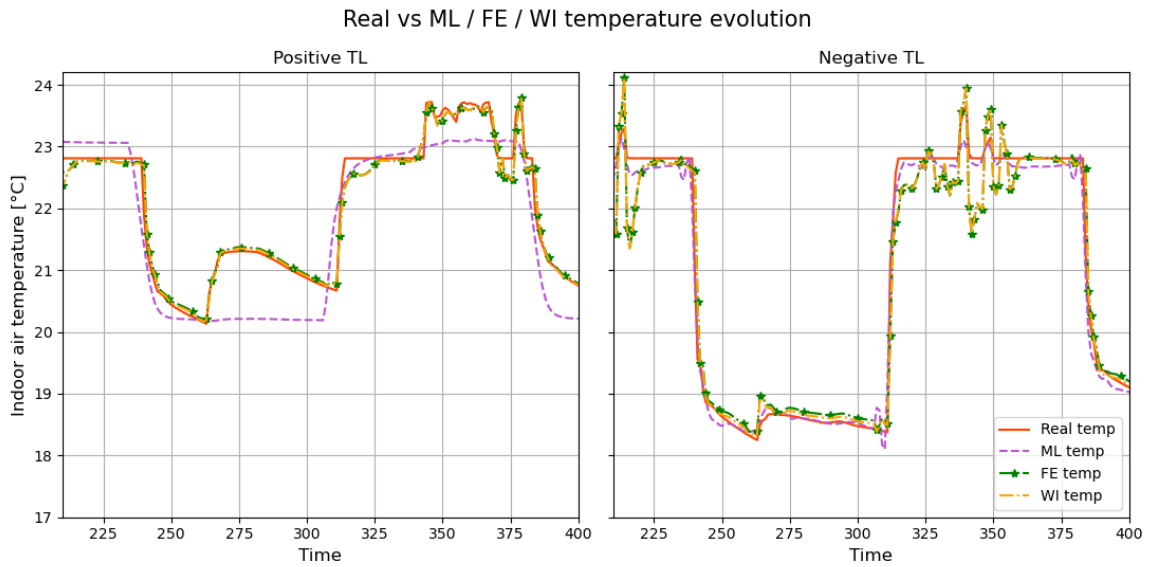
Fig. 5.18: Real temperature evolution vs ML/TL-FE/TL-WI one.

When positive TL occurs, it is clear that ML technique isn't able to follow the real temperature evolution and, consequently, in this case the building dynamics prediction can't be implemented in a MPC the control strategy applications. Thus, if a new building is erected or an energy requalification with new meters installation are applied, both transfer learning applications are needed to realize a building automation system providing high prediction accuracy and efficient control strategies.

Chapter 6

Conclusions

This thesis work provides a feasibility analysis of the transfer learning application on building dynamic issue, comparing it with traditional machine learning technique. In particular, two types of transfer learning methods are taken into account: *weights initialization* and *feature extraction*. The study examines more than 250 building boundary conditions configurations to rank features that affect the models performance, choosing at the beginning a source case. In addiction to the technique methods exploited, features taken into account are the climate type, the efficiency level in terms of building insulation, the occupancy profile and the orientation of different zones. The analysis concerns not only a features classification, but has the further goal of understanding the data availability needed to forecast 1 hour ahead of indoor air temperature with high accuracy to allow a cost effective and better building energy control strategy. In this case, training periods of 1 week, 1 month and 1 year are considered. Before run the simulations, the neural network has to be selected. Two NNs types has been compared: a Multlayer Perceptron (MLP) and a Long-Short Term Memory (LSTM). An optimization process, through OPTUNA library, has been applied to get the better performance from both the nets and, at the of the process, the LSTM provides the best prediction accuracy. Thus, this

one has been exploited to run all simulations needed to the analysis. At the end of the simulation process, variables was examined and a statistical investigation of results was carried on. First of all, three different zones were comparing and results demonstrated that, although the zone purpose is the same respect to the source zone one, the orientation affects the model significantly, resulting the ML better than TL in a specific case. Then, the other features previously cited were examined, creating more than 250 boundary conditions configuration on the source zone. Metrics evaluation demonstrated that TL application provides better performance than ML method in more than 80% of cases. Moreover, results showed that the climate variable plays a crucial role on prediction outcomes because, testing the model on a climate type too dissimilar from the source one, the NN could be deceived without understanding right features relationship. In addiction, analysis proved that a training process on a monthly data availability aims the lowest metrics respect to the other two training period of which the yearly one is the worse. A statistical investigation, through regression and classification trees, indicated that efficiency level and occupancy profiles have a secondary role on prediction results, after technique exploited, climate type and data availability. From all analysis executed in this thesis work, follows that a possible solution and future challenge to ensure high building dynamics prediction performance, is create as many networks as similar climate type groups, to training the model on more uniform boundary conditions.

Appendix A

Table 1: Crossing cases simulations.

Climate	Efficiency	Occupancy	Technique	Training period	Testing period	Epochs	Format
1A	Low	run1	ML	1y	1y	90	
1A	Low	run1	ML	1m	1m	90	
1A	Low	run1	ML	1w	1w	90	
1A	Low	run1	FE	1y	1y	80	
1A	Low	run1	WI	1y	1y	80	1A-LE-O1
1A	Low	run1	WI	1y	1m	80	
1A	Low	run1	FE	1y	1w	80	
1A	Low	run1	WI	1y	1y	80	
1A	Low	run1	FE	1y	1m	80	
1A	Low	run1	WI	1y	1w	80	
1A	Standard	run1	ML	1y	1y	90	
1A	Standard	run1	ML	1m	1m	90	
1A	Standard	run1	ML	1w	1w	90	
1A	Standard	run1	FE	1y	1y	80	
1A	Standard	run1	WI	1y	1m	80	1A-SE-O1
1A	Standard	run1	FE	1y	1w	80	
1A	Standard	run1	WI	1y	1y	80	
1A	Standard	run1	FE	1y	1m	80	
1A	Standard	run1	WI	1y	1w	80	
1A	High	run-1	ML	1y	1y	90	
1A	High	run-1	ML	1m	1m	90	
1A	High	run-1	ML	1w	1w	90	
1A	High	run-1	FE	1y	1y	80	
1A	High	run-1	WI	1y	1m	80	1A-HE-O1

1A	High	run-1	FE	1y	1w	80	
1A	High	run-1	WI	1y	1y	80	
1A	High	run-1	FE	1y	1m	80	
1A	High	run-1	WI	1y	1w	80	
3C	Low	run-1	ML	1y	1y	90	
3C	Low	run-1	ML	1m	1m	90	
3C	Low	run-1	ML	1w	1w	90	
3C	Low	run-1	FE	1y	1y	80	
3C	Low	run-1	WI	1y	1m	80	3C-LE-O1
3C	Low	run-1	FE	1y	1w	80	
3C	Low	run-1	WI	1y	1y	80	
3C	Low	run-1	FE	1y	1m	80	
3C	Low	run-1	WI	1y	1w	80	
3C	Standard	run-1	ML	1y	1y	90	
3C	Standard	run-1	ML	1m	1m	90	
3C	Standard	run-1	ML	1w	1w	90	
3C	Standard	run-1	FE	1y	1y	80	
3C	Standard	run-1	WI	1y	1m	80	3C-SE-O1
3C	Standard	run-1	FE	1y	1w	80	
3C	Standard	run-1	WI	1y	1y	80	
3C	Standard	run-1	FE	1y	1m	80	
3C	Standard	run-1	WI	1y	1w	80	
3C	High	run-1	ML	1y	1y	90	
3C	High	run-1	ML	1m	1m	90	
3C	High	run-1	ML	1w	1w	90	
3C	High	run-1	FE	1y	1y	80	
3C	High	run-1	WI	1y	1m	80	3C-HE-O1
3C	High	run-1	FE	1y	1w	80	
3C	High	run-1	WI	1y	1y	80	
3C	High	run-1	FE	1y	1m	80	
3C	High	run-1	WI	1y	1w	80	
5A	Low	run-1	ML	1y	1y	90	
5A	Low	run-1	ML	1m	1m	90	
5A	Low	run-1	ML	1w	1w	90	
5A	Low	run-1	FE	1y	1y	80	

5A-LE-O1

5A	Low	run-1	WI	1y	1m	80	
5A	Low	run-1	FE	1y	1w	80	
5A	Low	run-1	WI	1y	1y	80	
5A	Low	run-1	FE	1y	1m	80	
5A	Low	run-1	WI	1y	1w	80	
5A	Standard	run-1	ML	1y	1y	90	
5A	Standard	run-1	ML	1m	1m	90	
5A	Standard	run-1	ML	1w	1w	90	
5A	Standard	run-1	FE	1y	1y	80	
5A	Standard	run-1	WI	1y	1m	80	5A-SE-O1
5A	Standard	run-1	FE	1y	1w	80	
5A	Standard	run-1	WI	1y	1y	80	
5A	Standard	run-1	FE	1y	1m	80	
5A	Standard	run-1	WI	1y	1w	80	
5A	High	run-1	ML	1y	1y	90	
5A	High	run-1	ML	1m	1m	90	
5A	High	run-1	ML	1w	1w	90	
5A	High	run-1	FE	1y	1y	80	
5A	High	run-1	WI	1y	1m	80	5A-HE-O1
5A	High	run-1	FE	1y	1w	80	
5A	High	run-1	WI	1y	1y	80	
5A	High	run-1	FE	1y	1m	80	
5A	High	run-1	WI	1y	1w	80	
1A	High	run-1	ML	1y	1y	90	
1A	High	run-1	ML	1m	1m	90	
1A	High	run-1	ML	1w	1w	90	
1A	High	run-1	FE	1y	1y	80	
1A	High	run-1	WI	1y	1m	80	1A-HE-O1
1A	High	run-1	FE	1y	1w	80	
1A	High	run-1	WI	1y	1y	80	
1A	High	run-1	FE	1y	1m	80	
1A	High	run-1	WI	1y	1w	80	
3C	Low	run-1	ML	1y	1y	90	
3C	Low	run-1	ML	1m	1m	90	
3C	Low	run-1	ML	1w	1w	90	

3C-LE-O1

3C	Low	run-1	FE	1y	1y	80	
3C	Low	run-1	WI	1y	1m	80	
3C	Low	run-1	FE	1y	1w	80	
3C	Low	run-1	WI	1y	1y	80	
3C	Low	run-1	FE	1y	1m	80	
3C	Low	run-1	WI	1y	1w	80	
3C	Standard	run-1	ML	1y	1y	90	
3C	Standard	run-1	ML	1m	1m	90	
3C	Standard	run-1	ML	1w	1w	90	
3C	Standard	run-1	FE	1y	1y	80	
3C	Standard	run-1	WI	1y	1m	80	3C-SE-O1
3C	Standard	run-1	FE	1y	1w	80	
3C	Standard	run-1	WI	1y	1y	80	
3C	Standard	run-1	FE	1y	1m	80	
3C	Standard	run-1	WI	1y	1w	80	
3C	High	run-1	ML	1y	1y	90	
3C	High	run-1	ML	1m	1m	90	
3C	High	run-1	ML	1w	1w	90	
3C	High	run-1	FE	1y	1y	80	
3C	High	run-1	WI	1y	1m	80	3C-HE-O1
3C	High	run-1	FE	1y	1w	80	
3C	High	run-1	WI	1y	1y	80	
3C	High	run-1	FE	1y	1m	80	
3C	High	run-1	WI	1y	1w	80	
5A	Low	run-1	ML	1y	1y	90	
5A	Low	run-1	ML	1m	1m	90	
5A	Low	run-1	ML	1w	1w	90	
5A	Low	run-1	FE	1y	1y	80	
5A	Low	run-1	WI	1y	1m	80	5A-LE-O1
5A	Low	run-1	FE	1y	1w	80	
5A	Low	run-1	WI	1y	1y	80	
5A	Low	run-1	FE	1y	1m	80	
5A	Low	run-1	WI	1y	1w	80	
5A	Standard	run-1	ML	1y	1y	90	
5A	Standard	run-1	ML	1m	1m	90	

5A	Standard	run-1	ML	1w	1w	90	
5A	Standard	run-1	FE	1y	1y	80	
5A	Standard	run-1	WI	1y	1m	80	
5A	Standard	run-1	FE	1y	1w	80	
5A	Standard	run-1	WI	1y	1y	80	
5A	Standard	run-1	FE	1y	1m	80	
5A	Standard	run-1	WI	1y	1w	80	
5A	High	run-1	ML	1y	1y	90	
5A	High	run-1	ML	1m	1m	90	
5A	High	run-1	ML	1w	1w	90	
5A	High	run-1	FE	1y	1y	80	
5A	High	run-1	WI	1y	1m	80	5A-HE-O1
5A	High	run-1	FE	1y	1w	80	
5A	High	run-1	WI	1y	1y	80	
5A	High	run-1	FE	1y	1m	80	
5A	High	run-1	WI	1y	1w	80	
1A	Low	run-2	ML	1y	1y	90	
1A	Low	run-2	ML	1m	1m	90	
1A	Low	run-2	ML	1w	1w	90	
1A	Low	run-2	FE	1y	1y	80	
1A	Low	run-2	WI	1y	1m	80	1A-LE-O2
1A	Low	run-2	FE	1y	1w	80	
1A	Low	run-2	WI	1y	1y	80	
1A	Low	run-2	FE	1y	1m	80	
1A	Low	run-2	WI	1y	1w	80	
1A	Standard	run-2	ML	1y	1y	90	
1A	Standard	run-2	ML	1m	1m	90	
1A	Standard	run-2	ML	1w	1w	90	
1A	Standard	run-2	FE	1y	1y	80	
1A	Standard	run-2	WI	1y	1m	80	1A-SE-O2
1A	Standard	run-2	FE	1y	1w	80	
1A	Standard	run-2	WI	1y	1y	80	
1A	Standard	run-2	FE	1y	1m	80	
1A	Standard	run-2	WI	1y	1w	80	
1A	High	run-2	ML	1y	1y	90	

1A-HE-O2

1A	High	run-2	ML	1m	1m	90	
1A	High	run-2	ML	1w	1w	90	
1A	High	run-2	FE	1y	1y	80	
1A	High	run-2	WI	1y	1m	80	
1A	High	run-2	FE	1y	1w	80	
1A	High	run-2	WI	1y	1y	80	
1A	High	run-2	FE	1y	1m	80	
1A	High	run-2	WI	1y	1w	80	
3C	Low	run-2	ML	1y	1y	90	
3C	Low	run-2	ML	1m	1m	90	
3C	Low	run-2	ML	1w	1w	90	
3C	Low	run-2	FE	1y	1y	80	
3C	Low	run-2	WI	1y	1m	80	3C-LE-O2
3C	Low	run-2	FE	1y	1w	80	
3C	Low	run-2	WI	1y	1y	80	
3C	Low	run-2	FE	1y	1m	80	
3C	Low	run-2	WI	1y	1w	80	
3C	Standard	run-2	ML	1y	1y	90	
3C	Standard	run-2	ML	1m	1m	90	
3C	Standard	run-2	ML	1w	1w	90	
3C	Standard	run-2	FE	1y	1y	80	
3C	Standard	run-2	WI	1y	1m	80	3C-SE-O2
3C	Standard	run-2	FE	1y	1w	80	
3C	Standard	run-2	WI	1y	1y	80	
3C	Standard	run-2	FE	1y	1m	80	
3C	Standard	run-2	WI	1y	1w	80	
3C	High	run-2	ML	1y	1y	90	
3C	High	run-2	ML	1m	1m	90	
3C	High	run-2	ML	1w	1w	90	
3C	High	run-2	FE	1y	1y	80	
3C	High	run-2	WI	1y	1m	80	3C-HE-O2
3C	High	run-2	FE	1y	1w	80	
3C	High	run-2	WI	1y	1y	80	
3C	High	run-2	FE	1y	1m	80	
3C	High	run-2	WI	1y	1w	80	

5A	Low	run-2	ML	1y	1y	90	
5A	Low	run-2	ML	1m	1m	90	
5A	Low	run-2	ML	1w	1w	90	
5A	Low	run-2	FE	1y	1y	80	
5A	Low	run-2	WI	1y	1m	80	5A-LE-O2
5A	Low	run-2	FE	1y	1w	80	
5A	Low	run-2	WI	1y	1y	80	
5A	Low	run-2	FE	1y	1m	80	
5A	Low	run-2	WI	1y	1w	80	
5A	Standard	run-2	ML	1y	1y	90	
5A	Standard	run-2	ML	1m	1m	90	
5A	Standard	run-2	ML	1w	1w	90	
5A	Standard	run-2	FE	1y	1y	80	
5A	Standard	run-2	WI	1y	1m	80	5A-SE-O2
5A	Standard	run-2	FE	1y	1w	80	
5A	Standard	run-2	WI	1y	1y	80	
5A	Standard	run-2	FE	1y	1m	80	
5A	Standard	run-2	WI	1y	1w	80	
5A	High	run-2	ML	1y	1y	90	
5A	High	run-2	ML	1m	1m	90	
5A	High	run-2	ML	1w	1w	90	
5A	High	run-2	FE	1y	1y	80	
5A	High	run-2	WI	1y	1m	80	5A-HE-O2
5A	High	run-2	FE	1y	1w	80	
5A	High	run-2	WI	1y	1y	80	
5A	High	run-2	FE	1y	1m	80	
5A	High	run-2	WI	1y	1w	80	
1A	Low	run-3	ML	1y	1y	90	
1A	Low	run-3	ML	1m	1m	90	
1A	Low	run-3	ML	1w	1w	90	
1A	Low	run-3	FE	1y	1y	80	
1A	Low	run-3	WI	1y	1m	80	1A-LE-O3
1A	Low	run-3	FE	1y	1w	80	
1A	Low	run-3	WI	1y	1y	80	

1A	Low	run-3	FE	1y	1m	80	
1A	Low	run-3	WI	1y	1w	80	
1A	Standard	run-3	ML	1y	1y	90	
1A	Standard	run-3	ML	1m	1m	90	
1A	Standard	run-3	ML	1w	1w	90	
1A	Standard	run-3	FE	1y	1y	80	
1A	Standard	run-3	WI	1y	1m	80	1A-SE-O3
1A	Standard	run-3	FE	1y	1w	80	
1A	Standard	run-3	WI	1y	1y	80	
1A	Standard	run-3	FE	1y	1m	80	
1A	Standard	run-3	WI	1y	1w	80	
1A	High	run-3	ML	1y	1y	90	
1A	High	run-3	ML	1m	1m	90	
1A	High	run-3	ML	1w	1w	90	
1A	High	run-3	FE	1y	1y	80	
1A	High	run-3	WI	1y	1m	80	1A-HE-O3
1A	High	run-3	FE	1y	1w	80	
1A	High	run-3	WI	1y	1y	80	
1A	High	run-3	FE	1y	1m	80	
1A	High	run-3	WI	1y	1w	80	
3C	Low	run-3	ML	1y	1y	90	
3C	Low	run-3	ML	1m	1m	90	
3C	Low	run-3	ML	1w	1w	90	
3C	Low	run-3	FE	1y	1y	80	
3C	Low	run-3	WI	1y	1m	80	3C-LE-O3
3C	Low	run-3	FE	1y	1w	80	
3C	Low	run-3	WI	1y	1y	80	
3C	Low	run-3	FE	1y	1m	80	
3C	Low	run-3	WI	1y	1w	80	
3C	Standard	run-3	ML	1y	1y	90	
3C	Standard	run-3	ML	1m	1m	90	
3C	Standard	run-3	ML	1w	1w	90	
3C	Standard	run-3	FE	1y	1y	80	
3C	Standard	run-3	WI	1y	1m	80	3C-SE-O3
3C	Standard	run-3	FE	1y	1w	80	

3C	Standard	run-3	WI	1y	1y	80	
3C	Standard	run-3	FE	1y	1m	80	
3C	Standard	run-3	WI	1y	1w	80	
3C	High	run-3	ML	1y	1y	90	
3C	High	run-3	ML	1m	1m	90	
3C	High	run-3	ML	1w	1w	90	
3C	High	run-3	FE	1y	1y	80	
3C	High	run-3	WI	1y	1m	80	3C-HE-O3
3C	High	run-3	FE	1y	1w	80	
3C	High	run-3	WI	1y	1y	80	
3C	High	run-3	FE	1y	1m	80	
3C	High	run-3	WI	1y	1w	80	
5A	Low	run-3	ML	1y	1y	90	
5A	Low	run-3	ML	1m	1m	90	
5A	Low	run-3	ML	1w	1w	90	
5A	Low	run-3	FE	1y	1y	80	
5A	Low	run-3	WI	1y	1m	80	5A-LE-O3
5A	Low	run-3	FE	1y	1w	80	
5A	Low	run-3	WI	1y	1y	80	
5A	Low	run-3	FE	1y	1m	80	
5A	Low	run-3	WI	1y	1w	80	
5A	Standard	run-3	ML	1y	1y	90	
5A	Standard	run-3	ML	1m	1m	90	
5A	Standard	run-3	ML	1w	1w	90	
5A	Standard	run-3	FE	1y	1y	80	
5A	Standard	run-3	WI	1y	1m	80	5A-SE-O3
5A	Standard	run-3	FE	1y	1w	80	
5A	Standard	run-3	WI	1y	1y	80	
5A	Standard	run-3	FE	1y	1m	80	
5A	Standard	run-3	WI	1y	1w	80	
5A	High	run-3	ML	1y	1y	90	
5A	High	run-3	ML	1m	1m	90	
5A	High	run-3	ML	1w	1w	90	
5A	High	run-3	FE	1y	1y	80	
5A	High	run-3	WI	1y	1m	80	5A-HE-O3

5A	High	run-3	FE	1y	1w	80	
5A	High	run-3	WI	1y	1y	80	
5A	High	run-3	FE	1y	1m	80	
5A	High	run-3	WI	1y	1w	80	
1A	Low	run-3	ML	1y	1y	90	
1A	Low	run-3	ML	1m	1m	90	
1A	Low	run-3	ML	1w	1w	90	
1A	Low	run-3	FE	1y	1y	80	
1A	Low	run-3	WI	1y	1m	80	1A-LE-O3
1A	Low	run-3	FE	1y	1w	80	
1A	Low	run-3	WI	1y	1y	80	
1A	Low	run-3	FE	1y	1m	80	
1A	Low	run-3	WI	1y	1w	80	
1A	Standard	run-3	ML	1y	1y	90	
1A	Standard	run-3	ML	1m	1m	90	
1A	Standard	run-3	ML	1w	1w	90	
1A	Standard	run-3	FE	1y	1y	80	
1A	Standard	run-3	WI	1y	1m	80	1A-SE-O3
1A	Standard	run-3	FE	1y	1w	80	
1A	Standard	run-3	WI	1y	1y	80	
1A	Standard	run-3	FE	1y	1m	80	
1A	Standard	run-3	WI	1y	1w	80	
1A	High	run-3	ML	1y	1y	90	
1A	High	run-3	ML	1m	1m	90	
1A	High	run-3	ML	1w	1w	90	
1A	High	run-3	FE	1y	1y	80	
1A	High	run-3	WI	1y	1m	80	1A-HE-O3
1A	High	run-3	FE	1y	1w	80	
1A	High	run-3	WI	1y	1y	80	
1A	High	run-3	FE	1y	1m	80	
1A	High	run-3	WI	1y	1w	80	
3C	Low	run-3	ML	1y	1y	90	
3C	Low	run-3	ML	1m	1m	90	
3C	Low	run-3	ML	1w	1w	90	
3C	Low	run-3	FE	1y	1y	80	
							3C-LE-O3

3C	Low	run-3	WI	1y	1m	80	
3C	Low	run-3	FE	1y	1w	80	
3C	Low	run-3	WI	1y	1y	80	
3C	Low	run-3	FE	1y	1m	80	
3C	Low	run-3	WI	1y	1w	80	
3C	Standard	run-3	ML	1y	1y	90	
3C	Standard	run-3	ML	1m	1m	90	
3C	Standard	run-3	ML	1w	1w	90	
3C	Standard	run-3	FE	1y	1y	80	
3C	Standard	run-3	WI	1y	1m	80	3C-SE-O3
3C	Standard	run-3	FE	1y	1w	80	
3C	Standard	run-3	WI	1y	1y	80	
3C	Standard	run-3	FE	1y	1m	80	
3C	Standard	run-3	WI	1y	1w	80	
3C	High	run-3	ML	1y	1y	90	
3C	High	run-3	ML	1m	1m	90	
3C	High	run-3	ML	1w	1w	90	
3C	High	run-3	FE	1y	1y	80	
3C	High	run-3	WI	1y	1m	80	3C-HE-O3
3C	High	run-3	FE	1y	1w	80	
3C	High	run-3	WI	1y	1y	80	
3C	High	run-3	FE	1y	1m	80	
3C	High	run-3	WI	1y	1w	80	
5A	Low	run-3	ML	1y	1y	90	
5A	Low	run-3	ML	1m	1m	90	
5A	Low	run-3	ML	1w	1w	90	
5A	Low	run-3	FE	1y	1y	80	
5A	Low	run-3	WI	1y	1m	80	5A-LE-O3
5A	Low	run-3	FE	1y	1w	80	
5A	Low	run-3	WI	1y	1y	80	
5A	Low	run-3	FE	1y	1m	80	
5A	Low	run-3	WI	1y	1w	80	
5A	Standard	run-3	ML	1y	1y	90	
5A	Standard	run-3	ML	1m	1m	90	
5A	Standard	run-3	ML	1w	1w	90	

5A	Standard	run-3	FE	1y	1y	80	
5A	Standard	run-3	WI	1y	1m	80	
5A	Standard	run-3	FE	1y	1w	80	
5A	Standard	run-3	WI	1y	1y	80	
5A	Standard	run-3	FE	1y	1m	80	
5A	Standard	run-3	WI	1y	1w	80	
5A	High	run-3	ML	1y	1y	90	
5A	High	run-3	ML	1m	1m	90	
5A	High	run-3	ML	1w	1w	90	
5A	High	run-3	FE	1y	1y	80	
5A	High	run-3	WI	1y	1m	80	5A-HE-O3
5A	High	run-3	FE	1y	1w	80	
5A	High	run-3	WI	1y	1y	80	
5A	High	run-3	FE	1y	1m	80	
5A	High	run-3	WI	1y	1w	80	

Bibliography

[1] IEA, "Energy consumption by sector," 2021.

[2] S. Bouckaert, A. F. Pales, C. McGlade, U. Remme, B. Wanner, L. Varro, D. D'Ambrosio, and T. Spencer, "Net zero by 2050: A roadmap for the global energy sector," 2021.

[3] A. Gopstein, C. Nguyen, C. O'Fallon, N. Hastings, D. Wollman, *et al.*, "Nist framework and roadmap for smart grid interoperability standards, release 4.0," *NIST Spec. Publ*, 2021.

[4] L. Fiorini and M. Aiello, "Energy management for user's thermal and power needs: A survey," *Energy Reports*, vol. 5, pp. 1048–1076, 2019.

[5] S. Fathi, R. Srinivasan, A. Fenner, and S. Fathi, "Machine learning applications in urban building energy performance forecasting: A systematic review," *Renewable and Sustainable Energy Reviews*, vol. 133, p. 110287, 2020.

[6] D. Deletto, *Data-driven coordinated building cluster energy management to enhance energy efficiency, comfort and grid stability.* PhD thesis, Politecnico di Torino, 2020.

[7] G. Pinto, Z. Wang, A. Roy, T. Hong, and A. Capozzoli, "Transfer learning for smart buildings: A critical review of algorithms, applications, and future perspectives," *Advances in Applied Energy*, vol. 5, p. 100084, 2022.

[8] H. Li, Z. Wang, and T. Hong, "A synthetic building operation dataset," *Scientific data*, vol. 8, no. 1, pp. 1–13, 2021.

[9] IEA, "The critical role of buildings," 2019, Pris.

[10] W. S. U. Myles R. Allen (UK), Opha Pauline Dube (Botswana), "Intergovernamental panel on climate change, cap.1, ipcc," 2021.

[11] IEA, "World energy outlook 2021," 2021.

[12] A.-D. Pham, N.-T. Ngo, T. T. Ha Truong, N.-T. Huynh, and N.-S. Truong, "Predicting energy consumption in multiple buildings using machine learning for improving energy efficiency and sustainability," *Journal of Cleaner Production*, vol. 260, p. 121082, 2020.

[13] K. Foteinaki, R. Li, T. Péan, C. Rode, and J. Salom, "Evaluation of energy flexibility of low-energy residential buildings connected to district heating," *Energy and Buildings*, vol. 213, p. 109804, 2020.

[14] K. Aduda, T. Labeodan, W. Zeiler, G. Boxem, and Y. Zhao, "Demand side flexibility: Potentials and building performance implications," *Sustainable cities and society*, vol. 22, pp. 146–163, 2016.

[15] V. Karki, *Determination of Effectiveness of Energy Management System in Buildings*. West Virginia University, 2021.

[16] H. Gabbar, *Energy Conservation in Residential, Commercial, and Industrial Facilities*. IEEE Press Series on Systems Science and Engineering, Wiley, 2018.

[17] J. S. Vardakas, N. Zorba, and C. V. Verikoukis, "A survey on demand response programs in smart grids: Pricing methods and optimization algorithms," *IEEE Communications Surveys & Tutorials*, vol. 17, no. 1, pp. 152–178, 2014.

[18] A. Chakrabarty, E. Maddalena, H. Qiao, and C. Laughman, "Scalable bayesian optimization for model calibration: Case study on coupled building and hvac dynamics," *Energy and Buildings*, vol. 253, p. 111460, 2021.

[19] C. Xu, H. Chen, J. Wang, Y. Guo, and Y. Yuan, "Improving prediction performance for indoor temperature in public buildings based on a novel deep learning method," *Building and Environment*, vol. 148, pp. 128–135, 2019.

[20] X. Shi, W. Lu, Y. Zhao, and P. Qin, "Prediction of indoor temperature and relative humidity based on cloud database by using an improved bp neural network in chongqing," *Ieee Access*, vol. 6, pp. 30559–30566, 2018.

[21] C. Sun, J. Chen, S. Cao, X. Gao, G. Xia, C. Qi, and X. Wu, "A dynamic control strategy of district heating substations based on online prediction and indoor temperature feedback," *Energy*, vol. 235, p. 121228, 2021.

[22] M. J. Ellis and V. Chinde, "An encoder–decoder lstm-based empc framework applied to a building hvac system," *Chemical Engineering Research and Design*, vol. 160, pp. 508–520, 2020.

[23] F. Mtibaa, K.-K. Nguyen, M. Azam, A. Papachristou, J.-S. Venne, and M. Cheriet, "Lstm-based indoor air temperature prediction framework for hvac systems in smart buildings," *Neural Computing and Applications*, vol. 32, no. 23, pp. 17569–17585, 2020.

[24] Z. Fang, N. Crimier, L. Scanu, A. Midelet, A. Alyafi, and B. Delinchant, "Multi-zone indoor temperature prediction with lstm-based sequence to sequence model," *Energy and Buildings*, vol. 245, p. 111053, 2021.

[25] Facebook, "Prophet, forecasting scale," 2017.

[26] Z. Afroz, T. Urmee, G. Shafiullah, and G. Higgins, "Real-time prediction model for indoor temperature in a commercial building," *Applied energy*, vol. 231, pp. 29–53, 2018.

[27] C. Tim, "Optuna, optimize your optimization," 2017.